REVISTA MATÉRIA V.28 N.2
ISSN 1517-7076 articles e20230058, 2023

An effect of nano-SiC with different dielectric mediums on AZ61/7.5% B_4C nanocomposites studied through electrical discharge machining and Taguchi based complex proportional assessment method

Sakthi Selvarasu[1], Mahendran Subramanian[1], Jayasuthahar Thangasamy[1]

[1]University College of Engineering, Department of Mechanical Engineering, 610204, Thirukkuvalai, Tamilnadu, India.
e-mail: sakthi.mech1990sss@gmail.com, mahendran200@gmail.com, jayasuthahar@gmail.com

ABSTRACT

Magnesium based nanocomposites are new lightweight and high-performance materials for potential applications in biomedical, electronics, aerospace and automotive sectors owing to their lower density when compared with aluminum-based materials and steel. This article discusses the effect of pulse duration, pulse interval, current, gap voltage on Surface Roughness (SR), Material Removal Rate (MRR) and Electrode Wear Rate (EWR) of AZ61/7.5% B_4C composites have been studied based on the different dielectric medium, kerosene, Electrical Discharge Machining (EDM) oil and nanosilicon carbide added EDM oil. The magnesium nanocomposites have been prepared through stir casting. The L16 orthogonal array has been selected based on the four factors with four levels. The Complex Proportional Assessment (COPRAS) method has been used to find the optimum process parameters. An overall analysis found that the AZ61/7.5% B_4C composites has produced high mechanical properties compared with 2.5, 5, and 10wt.% B_4C nanocomposites. The pulse duration has most influencing factor for affecting the MRR and SR using analysis of variance. The developed quadratic models have well fit with experimental values. Using COPRAS, the optimal parameters are observed to be a maximum of 0.00730 g/s MRR, a minimum of 0.00127 g/s EWR, and a SR of 3.196 µm. The nano-SiC powder with EDM oil has a higher improvement than that of kerosene and EDM oil. The nano-SiC mixed EDM oil produces an improved performance measure of 81% MRR, 55% EWR, and 47% SR.

Keywords: AZ61; Boron Carbide; Nano-SiC; EDM.

1. INTRODUCTION

Surface roughness, material removal and electrode wear are important reactions for Electrical Discharge Machining (EDM) in metals or difficult-to-cut materials/nanocomposites [1]. To overcome the traditional machining problems, the nontraditional machining like EDM is selected [2,3]. There are more strategies used previously to improve these responses. Various strategies are used, including micron or nano-sized powder added to dielectric fluid, dielectric medium type, electrode polarity, low frequency vibration, varying process parameters, cryogenic treatment of the electrode/workpiece,heat treatment of the electrode, magnetic field assisted [4], computational methods [5], statistical methods [6] and design of experiments [7]. The genetic algorithm (GA) [8,9] and Non-Dominated Sorting Genetic Algorithm (NSGA-II) [10,11] are global optimization technique used for machining Ti-6Al-4V [12-14], Inconel Alloy 625 [15] and hybrid composites [16,17]. In the past, hydrocarbon-based oil (kerosene) has been used as dielectric fluid. As a result, the hydrocarbon oil breakdown, hazardous carcinogens, carbon dioxide, carbon monoxide, benzene, and polycyclic aromatic hydrocarbons are released. Therefore, the produced gases are reducing human life time through inhalation. Also, in order to worry less about fire in machining or the production of toxic gases, EDM oil is recommended to mitigate the aforementioned issues. A structural material with a lower density is magnesium alloy [18]. Because of its low density and biocompatibility, magnesium alloy has been praised for its use as a bio-implant metal, reducing greenhouse gas emissions and fossil fuel depletion [19]. In this work, magnesium-based composites were chosen to improve magnesium's resistance to wear, mechanical properties, tribological properties, corrosion behavior, and performance measures. Magnesium alloys are widely applied in electronic components, and medical apparatus and devices due to their high electrical and thermal conductivity, good ductility and excellent wear resistance, fatigue strength, and bearing properties. Hence, the different addition of particle reinforcement with magnesium alloy is used. Graphene oxide, nano-SiC, TiC, graphite, and BN are commonly used particles [20]. Furthermore,

Corresponding Author: Sakthi Selvarasu Received on 20/02/2023 Accepted on 10/04/2023

DOI: https://doi.org/10.1590/1517-7076-RMAT-2023-0058

it is well known that ceramic-reinforced composite materials are difficult to machine due to the abrasive nature of the hard reinforcement particles, which can quicken tool wear. [21]. Compared to simple EDM, Powder Mixed Electric Discharge Machining (PMEDM) produced a better result [22]. PMEDM plays a minor role in magnesium composites due to poor machinability [23]. Scientists always use statistical-mathematical models to describe the link between process factors and machining features. This means that ideal cutting conditions must be found in order for this process to be cost-effective [24].

2. LITERATURE REVIEW

Researchers are primarily concentrating on machining process parameters nowadays so that there will be maximum productivity, minimal losses, and improved machined surface qualities. The MRR was studied with increasing pulse duration for AZ61+B_4C+SiC composites. The MRR was increased with a rising the pulse duration (T_{on}) due to the erosion [25]. The 1% Mg and 3% copper mixed with Al6061/rich husk ash composites were fabricated and studied by varying the process parameters and rice husk ash. It was found that MRR had increased. The MRR was slightly reduced when the rich husk ash was raised. The low flushing pressure, high pulse duration, and duty cycle provided the high MRR [26]. The EDM was used to create the 0.5 mm microholes in the 0.8 wt% and 1.2 wt% nano alumina reinforced with magnesium composites. On varying the pulse duration (T_{on}), pulse interval (T_{off}), servo voltage (SV), and speed, the SR was studied. It was found that the 0.8 wt% and 1.2 wt% nano alumina reinforced with magnesium composites had different optimum process parameters. Additionally, it was observed that Ton was directly related to SR [27]. The magnesium metal matrix composites were fabricated by varying the SiC reinforcement weight percentage and SiC doping percentage. The MRR and SR were studied by varying the T_{on}, T_{off}, and wire feed rate. The results showed that increasing the Ton with an increased the MRR and SR [28]. To investigate the effects of machining parameters on wire EDM, the Taguchi method was combined with the grey relation method. Machining a Mg-MMC that is strengthened with reduced graphene oxide to remove as much material as possible while leaving the surface as smooth as possible. It was found that 0.2 wt.% of r-GO, 23 µs pulse interval (T_{off}), and 40 µs Ton were used to obtain the maximum MRR with minimal SR value [29]. The Al-20 Mg_2Si MMCs were fabricated and circular holes were drilled by varying the process parameters for studying the MRR and electrode wear. It was observed that MRR increased with I, T_{on}, and gap voltage increased. The electrode wear ratio was decreased above 80 V gap voltages [30]. To improve the MRR and TWR of the 30% vol. SiC/Al 359 composite, the EDM process parameters are varied. Lexical goal programming and desirability functional analysis were used. It was found that 16A current, 190 µs pulse duration, and 200 µs pulse-off time produced 1.91 mg/s MRR and 0.006 mg/s TWR. Two optimization tools produced the same results [31]. A WC-Co composite was attempted to be machined using the EDM method. According to research, cobalt melts and evaporates before WC particles do because the melting and evaporation points of the essential elements in composite materials differ. The results show that the machining was unsteady [32]. Another investigation was done to study the cutting mechanism of 15–35 vol.% SiC/Al composites machined using EDM. According to the report, the matrix material was not fully melted to separate the SiC particles under the fine cutting condition. However, during rough machining, the matrix melted and the SiC particles disintegrated, leaving noSiC particles in the heat-affected zone [33]. The work studies an experimental examination of the MRR and the EWR of a hybrid MMC of Al7075 with 10 wt% of silicon carbide reinforcement particles and Mg nanoparticles. It was shown that as pulse duration increased, the value of MRR decreased. Additionally, it was shown that EWR rises as the duty cycle (DC) enhances. Increasing in duty cycle resulted in high EWR due to the high energy density [34]. Based on the MRR and the EWR, we searched for gas-assisted EDM, gas-assisted powder mixed EDM, and rotary EDM. Compared to rotary EDM, gas-assisted powder mixed EDM was up to 75% better at getting rid of metal and at least 25% better at reducing electrode wear [35]. The metal matrix nanocomposite, newly created Al 7075 with 1.5 wt.% SiC nanoparticle reinforcement, was fabricated using an advanced ultrasonic cavitation technique. By adjusting the current, voltage, pulse interval, and pulse duration the MRR, EWR, and SR were studied. The best voltage, pulse current, pulse duration, and pulse interval were found to be 50V, 8A, 8s, and 9s. This gave the highest MRR and the lowest EWR and SR [36]. An experimental examination of the tool wear rate was conducted in powder-mixed EDM of Al6061 alloy augmented with 10 wt% SiC particles. A4 g/l concentration of tungsten powder was added to the dielectric fluid. For the machining of AA6061/10wt% SiC composite, it was discovered that the powder-mixed EDM technique results in a 51.12% reduction in tool wear rate [37]. In comparison to pure dielectric, the MRR and surface quality of the EDM of aluminium reinforced with 10% SiCp were increased by 38.22 and 46.06 %, respectively, by the addition of multi walled carbon nanotubes to the dielectric [38]. In a different study, it was discovered that the dielectric medium mixed with the aluminium powder was employed to improve the SR and MRR [39,40]. Copper electrode was produced a good surface finish [41]. In the EDM process, an electrode with a higher melting temperature provides superior wear resistance. For instance, due to copper's greater melting

temperature than brass, its wear rate is lower [42]. In prior research work for EDM of Al/TiC MMC [43], Al/Al_2O_3 [44], Al/SiCp [45], and Al/SiCp [46], copper material was selected based on prior investigations. Optimization was a vital way to raise component productivity. So, an optimization technique was employed. To solve the single response, the Taguchi approach was used to examine the impact of input parameters on $Al6061/Al_2O_3$ MMC in EDM [47]. The central composite design was employed to assess EDM input factors on Al6061/4% Gr/10% SiC MMCs [48]. The quadratic models were used to determine the anticipated value. Input-output matrix connection modelling heavily relies on manual computing methods like quadratic models [49].

An extensive literature revealed that current is highly affecting the material removal rate, electrode wear rate and surface roughness of magnesium composites. No study has been conducted so far on EDM using kerosene, EDM oil and nano-SiC added EDM oil on AZ61 Mg/B_4C composites. The disadvantage of conventional kerosene gives more debris formation on the machined surface, high electrode wear, high crack intensity and high surface roughness. To check the conventional kerosene, EDM oil and nano-SiC added EDM oil performance have been used as novelties. In this work, an effort has been made to machine AZ61 Mg/B_4C composites using conventional kerosene, EDM oil and nano-SiC added EDM oil and the results obtained with kerosene are discussed. The present work aims to machine AZ61 Mg/B_4C composites carried out using an EDM with kerosene, EDM oil and nano-SiC added EDM oil. The lists of findings are given below.

The major findings are given below.

- The B_4C nanoparticles dispersed in AZ61 have been studied using FESEM images.
- The elements in machined surfaces have been detected using EDS analysis.
- The performance of different dielectric mediums has studied using interval plots.
- The EDM factors effect on MRR, EWR and SR of magnesium composites have been studied using mean graphs.
- The most significant factor has studied using analysis of variance.
- The quadratic models of MRR, EWR and SR have been developed using Microsoft Excel software.
- The model factors have been calculated to find the strength of the model.
- The COPRAS method has used to determine the optimum process parameters.
- The present results have been compared with previous works.

3. MATERIALS AND METHODS

3.1. Fabrication of nanocomposites

The Mg and Zn were used to make the AZ61 composites, which also contained 5% sulphur hexafluoride SF60 and were produced in a higher-frequency emitting furnace with protective gas. At first, the melting process was conducted in a crucible furnace by blaming pure Mg. Additionally, the AZ61 magnesium alloy was completely dissolved in molten magnesium. An unblended boron carbide particle with a grain size of 90nm was stir cast over the molten alloy in order to activate the composite in an off-site operation. The B_4C particle served as a reinforcing agent and was heated to 400°C in atmospheric conditions for two hours. A steel impeller was used to uniform mixing of particles. The various weight percentages of preheated B_4C particles (2.5, 5, 7.5, and 10) were added with the alloy AZ61 that was in a molten condition in a furnace as part of the stir casting process. In this 15minutes duration, the stir casting process was maintained at a 620 rpm stirring rate. The stirring duration and speed were obtained from previous articles on Mg-based MMCs [50]. Particles in the molten alloy were heated by the vortex method to 780ºC before being raised for 120 minutes at 400ºC. Ultimately, the composites of the liquefied alloy were tilted at temperature of 750°C in cylindrical, cast iron, preheated mould at a temperature of 100°C [51]. In order to study the microstructures, all cast samples were polished and etched using an acetic-picryl solution. The microstructure and EDS were studied for nanocomposites. The effects of B_4C nanoparticles dispersed in AZ61 were studied using FESEM images, which are shown in Figure 1 (a–e). The elements present in alloys and nanocomposites were studied using EDS reports, which are shown in Figure 2 (a–e).

3.2. Experimental procedure

The AZ61/7.5 wt.% B_4C nanocomposite with 1.8mm thickness was selected as a sample material compared with other 2.5, 5, and 10 wt.% B_4C nanocomposites. This was due to the high mechanical properties such as yield strength of 139 MPa, ultimate tensile strength of 195 MPa, hardness of 107 HV, compressive strength of 370 MPa, and impact strength of 28 J, which were found as per ASTM standards. In this study, the EDM machine was utilised to form a 0.8 mm square holes in the AZ61/7.5 wt.% B_4C nanocomposite by using copper electrodes

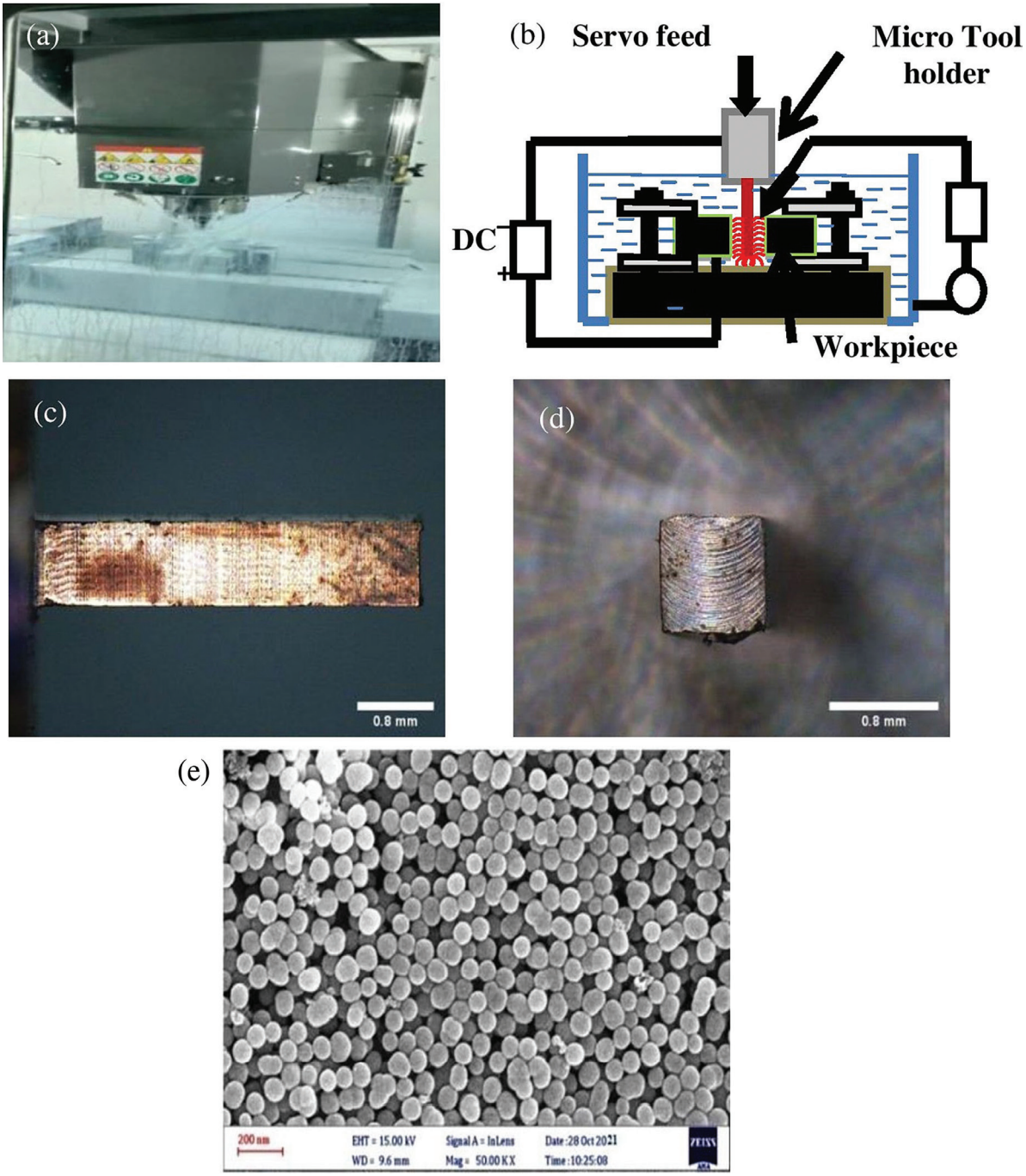

Figure 1: EDM setup (a), Schematic diagram of EDM setup (b), Front view of square electrode (c), Top view of square electrode (d) and nano-SiC particles (e).

with a dimension of 0.8 mm square. Boron carbide was the hardest element, which had a fracture toughness and high elastic modulus. The addition of Boron Carbide (B_4C) in the magnesium matrix increased the hybrid composite flexural strength, interfacial bonding strength, wear resistanceand hardness [52]. The 5mm diameter copper rod was reduced into 0.8 mm square electrodes by using a vertical machining center.Details of chemical compositions are shown in Table 1. Dielectric mediums such as kerosene, EDM oil, and nano-SiC mixed EDM oil were used in the dielectric medium as shown in Table 2. The 1.5 g/lit nano SiC was added to the dielectric medium per the recommendation of previous work [53]. Furthermore, according to trail tests, the positive electrode polarity was used. In EDM, pulse duration (T_{on}), pulse interval (T_{off}), Current (I) and Gap voltage (GV) were varied in EDM to improve the MRR of magnesium composite, EWR and the SR of the machined surface. Figure 1 shows the EDM setup, schematic line diagram of the EDM setup, square electrode in front view, square electrode in top view and nano SiC particles. Details of process parameters are shown in Table 3. Table 4

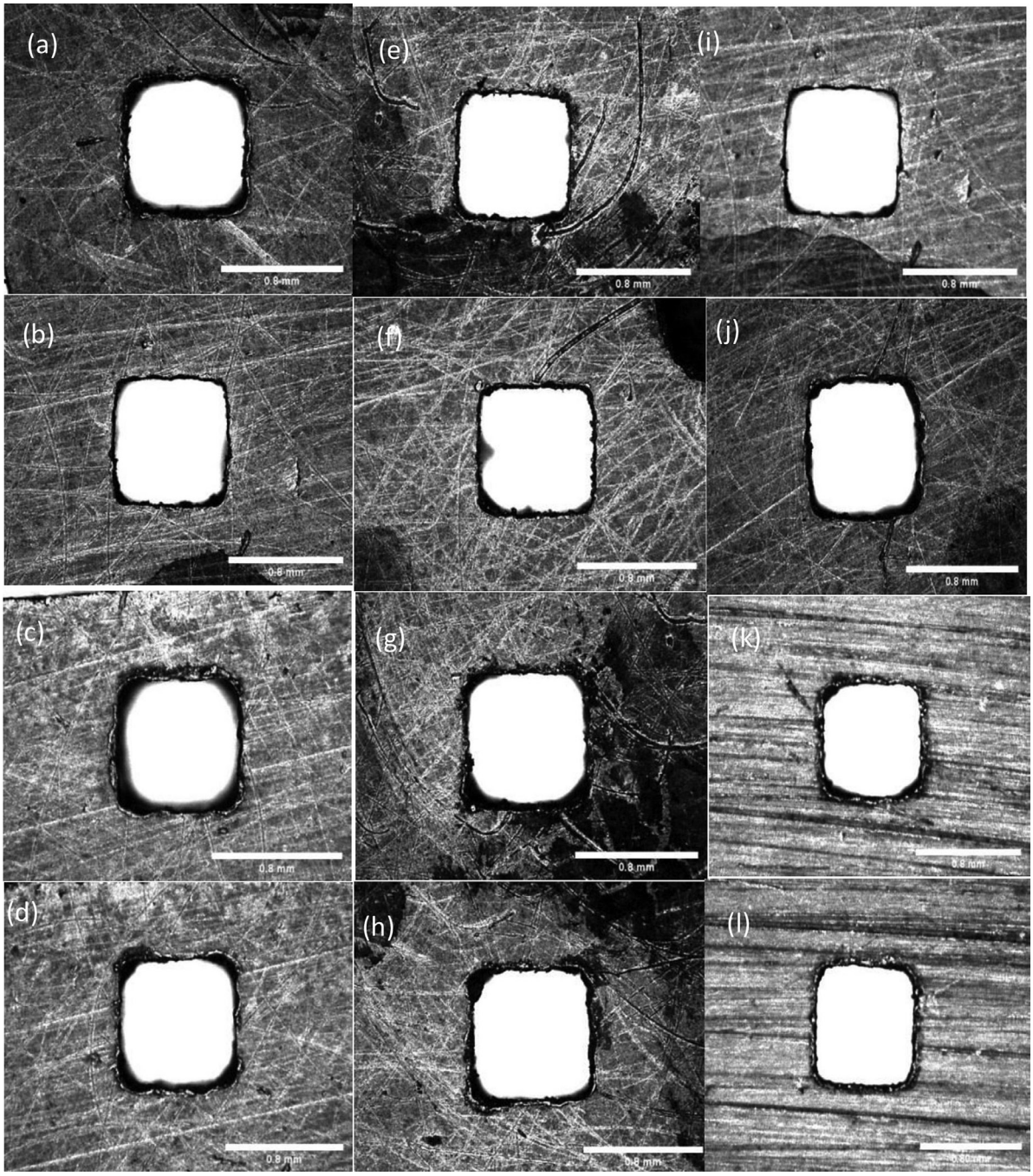

Figure 2: Machined holes: Kerosene (a)–(d), EDM oil (e)–(h) and SiC + EDM oil (i)–(l).

show the Taguchi design and experimental results for kerosene, EDM oil, and SiC + EDM oil. As per the design of experiments, the depth of square hole 1.8 mm was made on composites. Figure 2 shows the machined holes for kerosene, EDM oil, and nano-SiC + EDM oil. To find the best dielectric medium for machining of magnesium composite based on the MRR, EWR, and SR values, the interval plots were drawn using MINITAB software, which is shown in Figure 3. The ratio between the weight difference of work materials and machining time was calculated as MRR. An electronic balance with 0.0001 g precision was used to measure the weight. The machined holes were measured using a digital optical microscope and a scanning electron microscope. The MRR was calculated using equation (1).

$$MRR = (W1 - W2) \times 1000 \times \rho \times t \tag{1}$$

Where W1 and W2 are the workpiece's weights before and after the machining process, respectively (in grams), is the workpiece's density (in grams per cubic centimeter), and t is the machining time (in minutes).

Table 1: AZ61 and copper electrode chemical composition.

MATERIALS	ELEMENTS	MG	AL	ZN	MN	SI	CU	FE	NI
AZ61	Wt.%	Bal	6.73	1.0	0.21	0.03	0.003	0.0035	0.007
Materials	Elements	Cu	Bi	0	Pb	–	–	–	–
Copper	Wt.%	99.90	0.0005	0.040	0.005	–	–	–	–

Table 2: EDM oil, kerosene, SiC and B_4C properties.

PROPERTIES	KEROSENE	SiC	B_4C	EDM OIL
Density (kg/m^3)	860	3100	2520	835
Average particle size (nm)	–	85	100	–
Electrical conductivity (S/m)	50pS/m	70 - 140	100	400pS/m
Thermal conductivity (W/m K)	0.128	83.6	120 to 115	120
Specific heat (J/kg K)	2100	1040	950	1670
Melting point ($^{\circ}$C)	–	2730	2350	–
Hardness (HK)	–	2100–3000	33GPa	–

Table 3: Sectional of Process parameters and problems observed from the parameter levels.

FACTORS (UNITS/ SYMBOL)	PROBLEMS FOUND USING BELOW LIMITS	LEVELS				FROM THE LITERATURE PAPERS/ MACHINE LIMITS/ PROBLEMS FOUND USNG ABOVE LIMITS
		1	2	3	4	
Pulse duration ($\mu s/T_{on}$)	Electrode broken	20	40	60	80	On the basis of machine limit
Pulse interval ($\mu s/T_{off}$)	High SR	10	20	30	40	[28]
Current (A/I)	Electrode broken	2	4	6	8	[36]
Gap voltage (V/GV)	High process time	40	50	60	70	[30]

Similarly, EWR was also calculated. The surface roughness of the side wall of the machined surface was measured by the half-cut surface of a square hole, and a non-contact surface roughness tester was used.The trail test found that the mechanical properties of AZ61/7.5 wt.% B_4C nanocomposite is better than that of other combinations. Hence, AZ61/7.5 wt.% B_4C nanocomposite is selected further.

3.3. Quadratic model

The relation between the input and output in quadratic-order models was created using Microsoft Excel [54]. To determine the reliability of the data, which are also utilized for forecasts, the models have been applied.

$$Y = \beta_0 + \beta_1 T_{on} + \beta_2 I + \beta_3 T_{off} + \beta_4 GV + \beta_5 T_{on}^{\ 2} + \beta_6 I^2 + \beta_7 T_{off}^{\ 2} + \beta_8 GV^2 + \beta_9 T_{on} IT_{off} + \beta_{10} T_{on} IGV + \beta_{11} IT_{off} GV + \beta_{12} T_{off} GVT_{on} \quad (2)$$

Here Y = the predicted response. The coefficients are 1,...,12, and 0 is the constant. In order to assess the model strength, statistical indices are calculated [55].

Mean Absolute Percentage Error

$$MAPE = \left(\frac{1}{n}\right)\sum_{i=1}^{n}\left(\left(\left| C_{MActuali} - C_{MModeli} \right|\right) / C_{MActuali}\right) \times 100 \quad (3)$$

Table 4: Taguchi design and experimental results for kerosene, EDM Oil and SiC + EDMoil.

S. NO.	PROCESS PARAMETERS				MRR (g/s) (X 10^{-2})			EWR (g/s) (X 10^{-2})			SURFACE ROUGHNESS (μm)		
	T_{ON} (μS)	T_{OFF} (μS)	I (A)	GV (V)	KEROSENE	EDM OIL	SIC + EDM OIL	KEROSENE	EDM OIL	SIC + EDM OIL	KEROSENE	EDM OIL	SIC + EDM OIL
1	1	1	1	1	0.130	0.136	0.180	0.198	0.188	0.173	1.431	1.231	1.071
2	1	2	2	2	0.171	0.180	0.237	0.189	0.179	0.165	1.891	1.626	1.415
3	1	3	3	3	0.242	0.254	0.335	0.188	0.179	0.165	2.671	2.297	1.998
4	1	4	4	4	0.244	0.256	0.338	0.162	0.154	0.142	2.692	2.315	2.014
5	2	1	2	3	0.246	0.274	0.377	0.246	0.226	0.195	2.721	2.068	1.737
6	2	2	1	4	0.284	0.315	0.435	0.232	0.214	0.184	3.136	2.384	2.002
7	2	3	4	1	0.311	0.345	0.476	0.155	0.143	0.123	3.433	3.192	2.682
8	2	4	3	2	0.317	0.352	0.486	0.151	0.139	0.120	3.503	3.013	2.531
9	3	1	3	4	0.320	0.388	0.539	0.238	0.207	0.162	3.536	2.970	2.465
10	3	2	4	3	0.337	0.408	0.567	0.226	0.197	0.153	3.719	3.124	2.593
11	3	3	1	2	0.359	0.434	0.604	0.268	0.233	0.182	3.962	3.328	2.762
12	3	4	2	1	0.390	0.472	0.655	0.185	0.161	0.125	4.302	3.614	3.000
13	4	1	4	2	0.390	0.461	0.654	0.241	0.198	0.142	4.309	3.491	2.862
14	4	2	3	1	0.401	0.473	0.672	0.238	0.195	0.141	4.427	3.586	2.941
15	4	3	2	4	0.407	0.480	0.682	0.261	0.214	0.154	4.492	3.639	2.984
16	4	4	1	3	0.436	0.514	0.730	0.215	0.177	0.127	4.812	3.897	3.196

Root Mean Square Error

$$RMSE = \sqrt{\frac{1}{n}\sum_{i=1}^{n}\left(C_{MActuali} - C_{MModeli}\right)^2} \tag{4}$$

Coefficient of determination

$$R = 1 - \frac{\sum_{i=1}^{n}[(C_{Mobservedi} - \bar{C}_{Mobderved})]\ \left[(C_{Mpredictedi} - \bar{C}_{Mpredicted})\right]}{\sqrt{\sum_{i=1}^{n}(C_{Mactuali} - C_{MModeli})^2\ \sum_{i=1}^{n}(C_{Mpredictedi} - \bar{C}_{Mpredicted})^2}} \tag{5}$$

Here, the experimental values and the anticipated values are denoted by $C_{MActuali}$ and $C_{MModeli}$, respectively. The average value of the experimental model is represented by the notation $\bar{C}_{Mobserved}$ The number of observations is n as well.

3.4. The Complex Proportional Assessment (COPRAS)

The COPRAS approach was created by Zavadskas and Kaklauskas [56]. The optimal process parameters must be located in order to determine the best alternative utility degree, which is assessed using stepwise ranking.

The calculation steps are as.

Step 1: Formation of decision-making matrix

The values of the experimental data are chosen as criterion and are then organized into a matrix. The X_{IJ} matrix has m rows for options and n rows for criteria (columns). Each criterion is given a weight based on the aim.

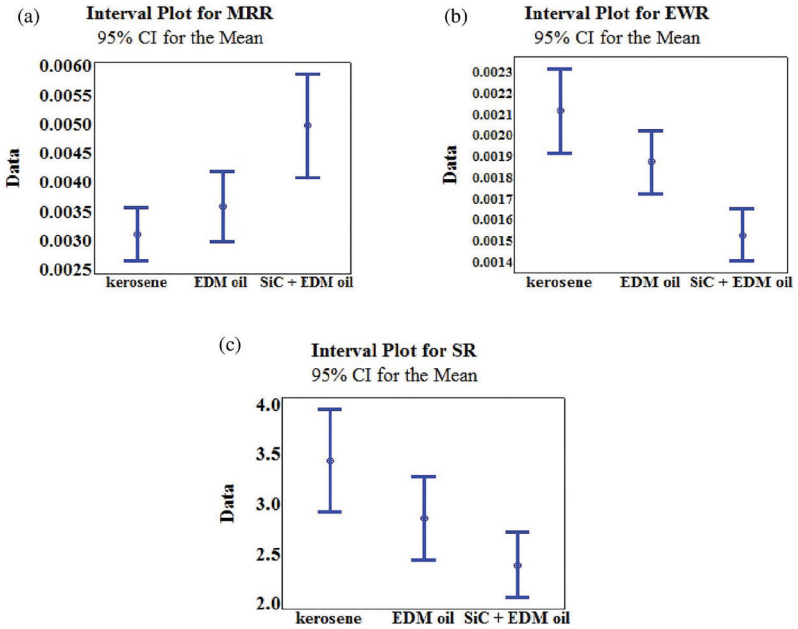

Figure 3: Interval plot for: MRR (**a**), EWR (**b**) and SR (**c**).

$$D = \begin{bmatrix} x_{11} & x_{12} \ldots & x_{1n} \\ x_{21} & x_{22} \ldots & x_{2n} \\ \vdots & \vdots\ \vdots & \vdots \\ \vdots & \vdots\ \vdots & \vdots \\ \vdots & \vdots \quad \vdots & \vdots \\ x_{m1} & x_{n2} \ldots & x_{mn} \end{bmatrix} \tag{6}$$

Here, j = 1,2,….,n; i = 0,1,…,m/

Step 2: Calculations are made to normalize the decision matrix and create a weighted-normalized decision matrix.

$$n_{ij} = \frac{x_{ij}}{\sum_{i=0}^{m} x_{ij}} \tag{7}$$

$$N_{ij} = W_{ij}\ x\ n_{ij} \tag{8}$$

Step 3: Calculate the value of the total of the benefit and cost criteria.

$$B_{ij} = \sum_{j=1}^{k} N_{ij} \tag{9}$$

$$C_i = \sum_{j=k+1}^{k} N_{ij} \tag{10}$$

Step 4: Determine the proportional importance of each option.

$$Q_i = B_i + \frac{\min(C_i) \times \sum_{i=1}^{n} C_i}{C_i \times \sum_{i=1}^{n} \left(\frac{\min\ (C_i)}{C_i} \right)} \tag{11}$$

Step 5: Degree of utility (UD) calculated for every alternative.

$$UD = \frac{Q_i}{\max(Q_i)} \times 100 \tag{12}$$

The greater the UD value, the better the alternative is found.

Step 6: UD values were used to rank the alternatives.

4. RESULTS AND DISCUSSIONS

4.1. Microstructure

The B_4C nanoparticles dispersed in AZ61 were studied using FESEM images, which are shown in Figure 4 (a–e). It was found that the nanoparticles were dispersed uniformly in the Mg matrix with white-coloured particles. The magnesium nanocomposite shows a dendritic feature through α-Mg in the matrix. The new intermetallic phase

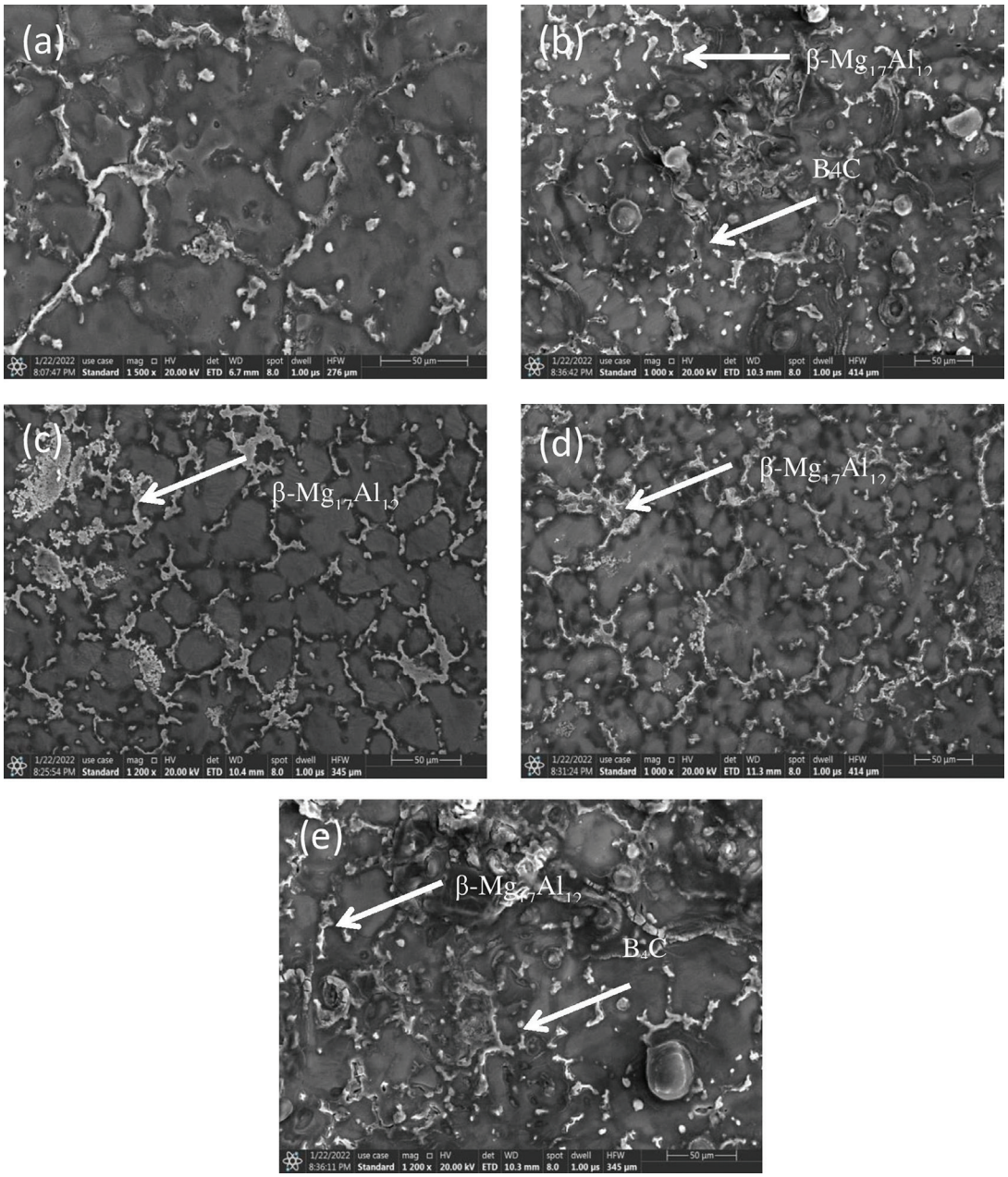

Figure 4: (a–e) AZ61/B_4C composites SEM analysis: (a) AZ61 alloy (b) AZ61/2.5 wt.% B_4C (c) AZ61/5 wt.% B_4C (d) AZ61/7.5 wt.% B_4C (e) AZ61/10 wt. % B_4C.

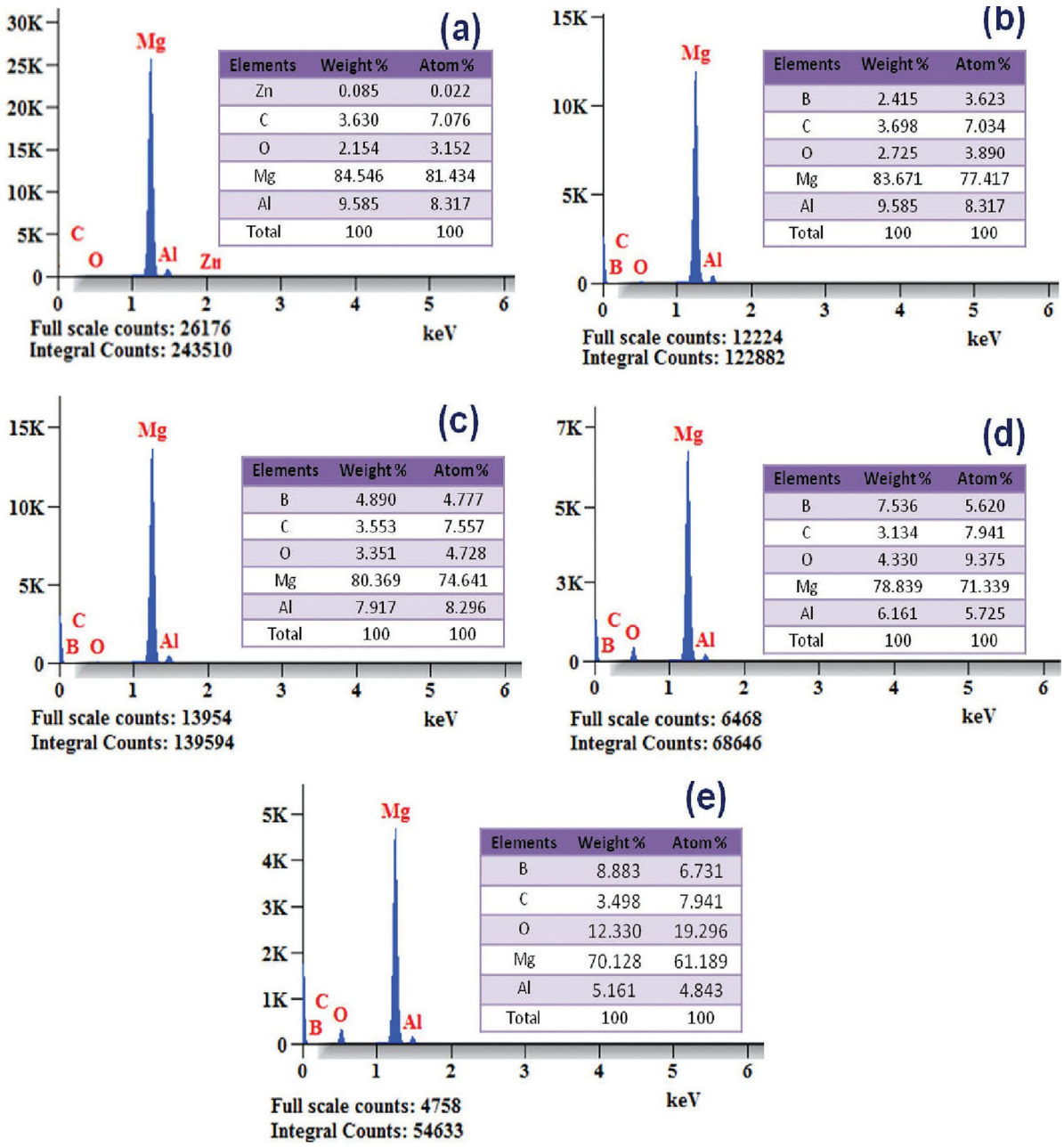

Figure 5: (a–e) AZ61/B_4C composites EDS analysis: (a) AZ61 alloy (b) AZ61/2.5wt.% B_4C (c) AZ61/5% wt.% B_4C (d) AZ61/7.5wt.% B_4C (e) AZ61/10wt.% B_4C.

β-$Mg_{17}Al_{12}$ was formed between the boundaries of Mg and B_4C particles. It was also found that no porosity was observed in the surface owing to the well stirring in the casting process. The 10 wt. % B_4C nanocomposite produced a cluster of particles as observed due to the non-isothermal heat reaction between the matrix and particle. The elements of surfaces were detected using EDS analysis, which is shown in Figure 5(a–e). It was confirmed that the elements present in nanocomposites (Mg, Al, B, and C) are similar to matrix and reinforced particles.

4.2. Material removal rate

Figure 6 shows that using EDM oil added with a SiC powder has a higher MRR than using kerosene and EDM oil. This was because SiC powder promotes EDM oil electrical conductivity. The gap was simultaneously enlarged to extrude the debris easily and SiC powder also disperses discharge energy, enhancing MRR efficiency. This was owing to gap extension during the machining process. The debris was easily removed from the gap and discharging energy dispersed during the machining process. Additionally, the result was due to the high thermal conductivity of SiC particles incorporated in the EDM oil attributed to the fact that generated heat uniformly dispersed throughout the machined surface. Because reinforcing particles in the base metal phase act

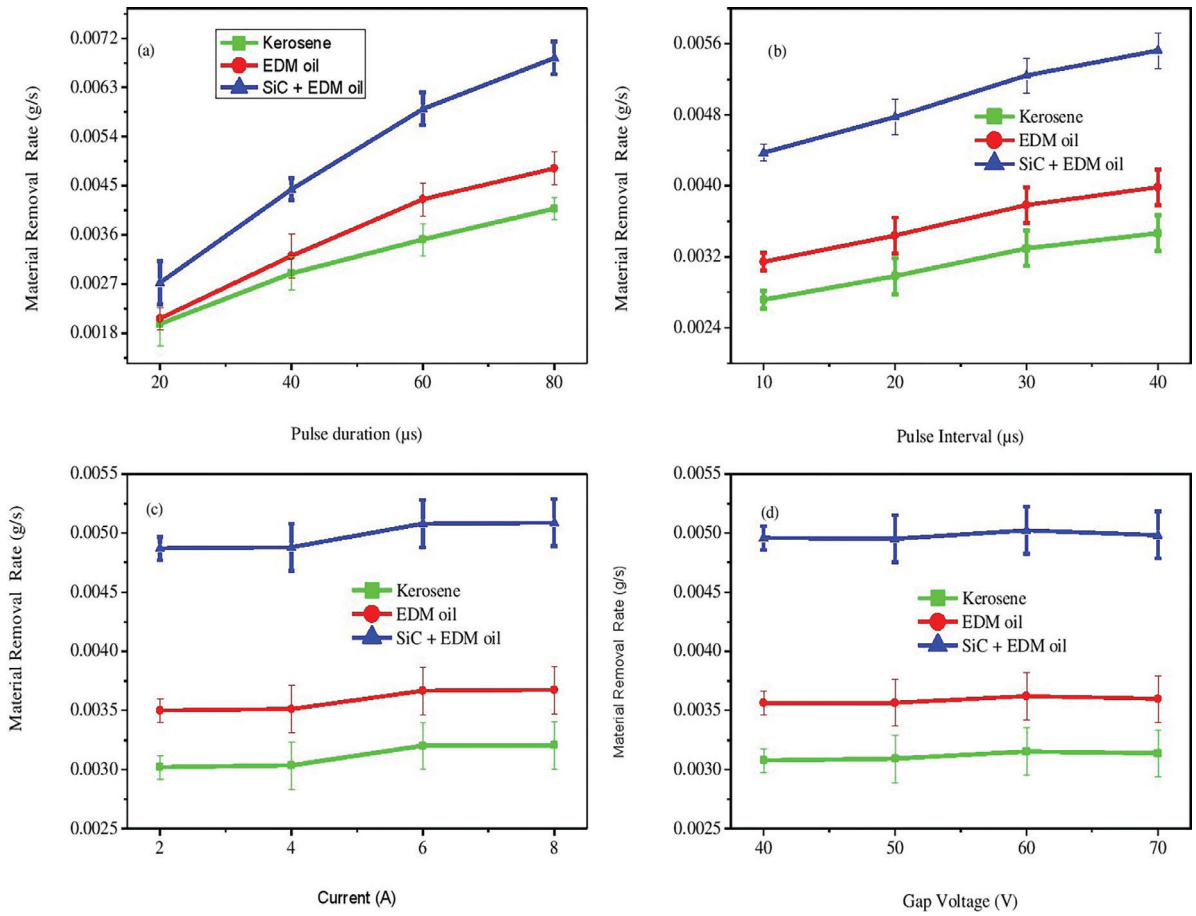

Figure 6: Effect of process parameters on MRR for Kerosene, EDM oil and SiC + EDM oil: (a) T_{on}, (b) T_{off}, (c) I and (d) GV.

as shields and protectors against sparks. As a result, Low volume fraction of reinforcing particles lead to increase in MRR. By reducing the size of the reinforcing particles in nanoscale, the MRR increased. Generally, the pulse duration was defined as the dielectric's breakdown voltage being observed, which caused its ionization. A spark between the electrode and the workpiece happened during the pause. The substance of the workpiece was subsequently eroded as a result of the spark. On increasing the pulse duration, MRR was increased owing to the high amount of heat energy generated on work materials [57]. Also, the MRR was increased with an increasing pulse interval and current. The voltage slightly affected the MRR. Compared to the performance of kerosene, the EDM oil exhibited better results owing to the high electrical with thermal conductivity of EDM oil. To improve the MRR for 30% vol. SiC/Al 359 composite, the EDM process parameters were varied. It was found that the optimum process parameters produced a 1.91 mg/s MRR. To compare the MRR for steel, Al, SiC, and Al_2O_3 powder added EDM, it was found that SiC powder added EDM produced a high MRR. The thermal conductivities of different powders did not have much influence on MRR compared with present results and it was identified in the past work [58]. Nevertheless, the present result showed that MRR was based on the thermal conductivity of powder. In reality, the sparking energy is directly proportional to Ton for improving the MRR. Similar trends were observed with increasing the pulse interval, current and gap voltage.

4.3. Electrode wear rate

The electrode wear rate was also an important response because it was affecting the performance measures. In EDM, zero electrode wear was unable to be achieved because of erosion of work material and electrode. Figure 7 depicts the effects of kerosene, EDM oil and nano-SiC added EDM oil on the EWR of copper electrodes. The correlation graphs drawn between the EWR and selected process factors are shown in Figure 8. In three different dielectric mediums, the SiC mixed EDM oil produced a better result due to less heat transfer in the electrode surface because of powders presented in the inner electrode gap absorbing heat during the process and transferred to the machined surface. Also, nano-SiC mixed EDM oil was used to increase spark gap and dielectric strength. Therefore, EWR was reduced compared with kerosene and EDM oil. The thermal conductivity of SiC particle was responsible for the event. As a result, heat produced during the machining was quickly

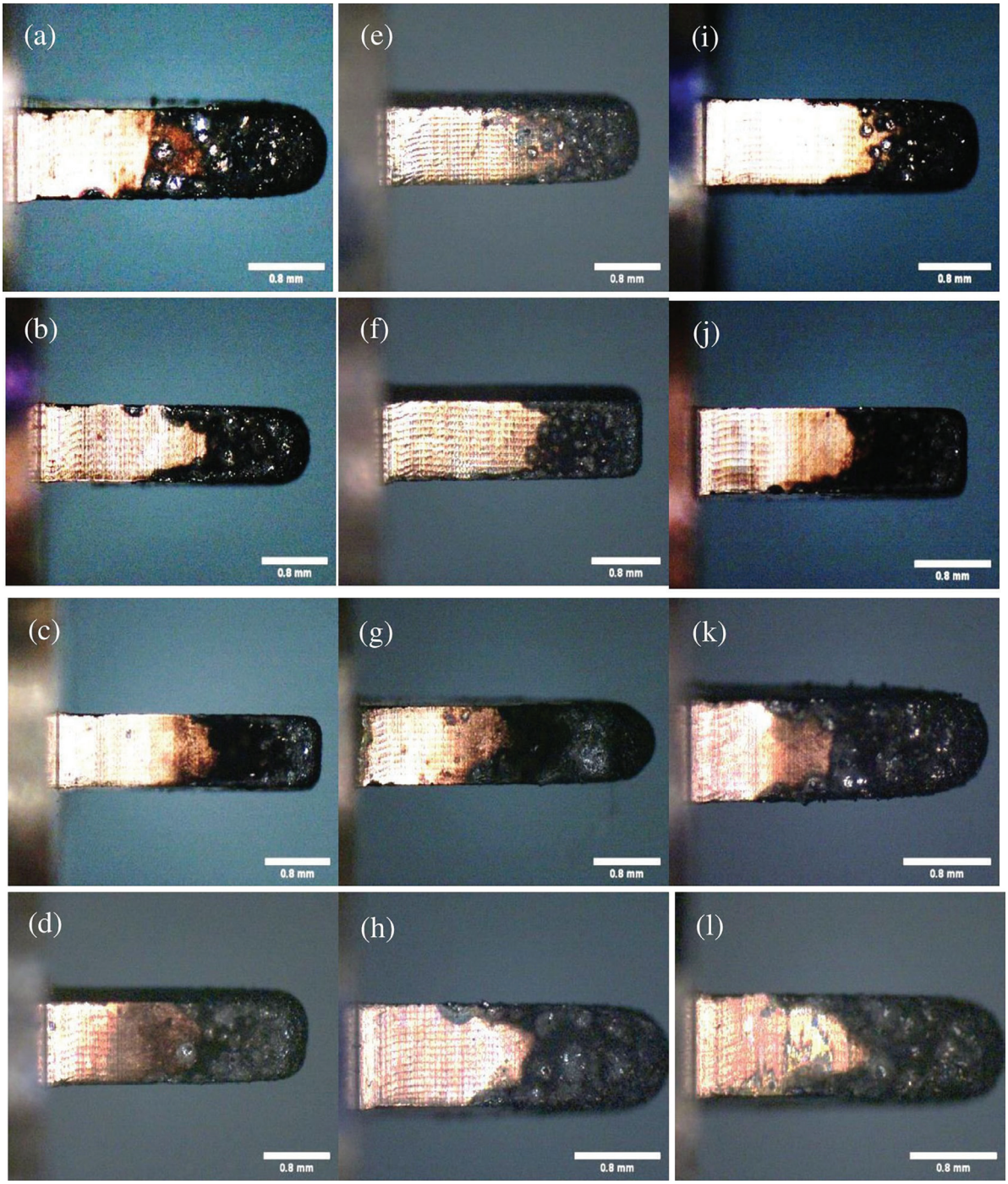

Figure 7: Machined Electrodes: Kerosene (**a**)–(**d**), EDM oil (**e**)–(**h**) and SiC + EDM oil (**i**)–(**l**).

dissipated. The heat removal makes it possible for the temperature to drop near the copper electrode surface for a long pulse duration, which lowered the EWR. The EWR was decreased with an increasing the pulse duration, pulse interval, and current. The MRR decreased with increasing pulse duration, as observed in previous work [58]. The addition of SiC powder with dielectric medium has a positive influence in the electrode wear. The result was owing to the presence of SiC with EDM oil, which provided a higher effect on EWR. The resistance of copper electrodes was increased with changing dielectric properties. With increasing pulse duration, the EWR fell in the opposite manner. Similar results were discovered in earlier research [59]. On increasing the current, the MRR was decreased. The reason for decreasing the EWR was the carbide deposits on the electrode surfaces. Similarly, on increasing the voltage, the MRR was increased. The reason for increasing the EWR was the loosened SiC deposits on the electrode surfaces.

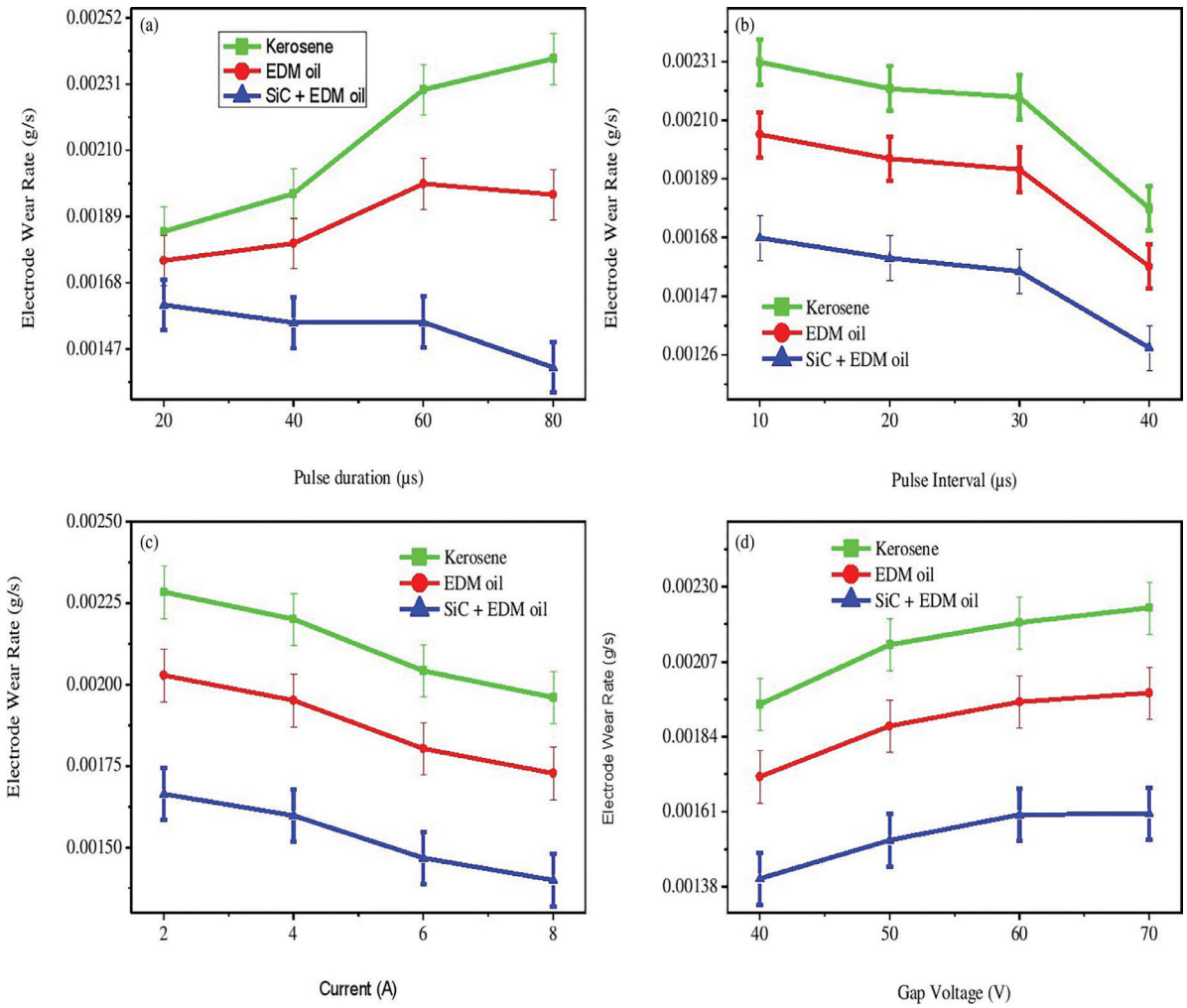

Figure 8: Effect of process parameters on EWR for Kerosene, EDM oil and SiC + EDM oil: (a) T_{on}, (b) T_{off}, (c) I and (d) GV.

4.4. Surface roughness

The surface roughness value was decided based on the crater size formation of the machined surface and selected process parameters. The correlation graphs drawn between the SR and selected process factors are shown in Figure 9. In different dielectric mediums, the addition of SiC powder particles with EDM oil was decreased the insulating strength of dielectric medium, as a result, an increase in the spark-gap distance between the electrode and workpiece material. Moreover, increasing in spark gap distance gave the surface a better polish and makes the process more stable. It also found that it easiest to flush debris in a uniform way. Thereby, the SiC mixed EDM oil produced a lower SR than kerosene and EDM oil when being machined. This resulted from the surface developing with fewer voids. The SiC added EDM oil was a higher electrical and thermal conductivity than that of kerosene. Hence, the SiC added EDM oil produced less SR. The crater formed with SiC-added EDM oil process had a smaller diameter and depth, resulting in a better surface finish. The surface roughness created when kerosene and EDM oil were used proportional to the size of the generated crate during EDM operations. The SR decreased with increasing the pulse duration, pulse interval, and current. This resulted in a bigger crater on the component surface. The result was owing to the increase in discharge energy. High Ton was used in the machining process to enlarge plasma channels, reduce energy densities, and create shallow craters on the surface [60]. The gap voltage did not much affect the SR using three different dielectric mediums. High current and long pulse duration result in increased heat energy released along with the formation of a bigger, hotter pool of molten metal. The molten substance explodes and forms gas bubbles as it is heated more intensely. High and deep craters result from this.

4.5. Analysis of variance

The statistical technique known as analysis of variances (ANOVA) examines the impact of one or more independent variables on a dependent variable of interest. It was a statistical formula that was used to assess variations

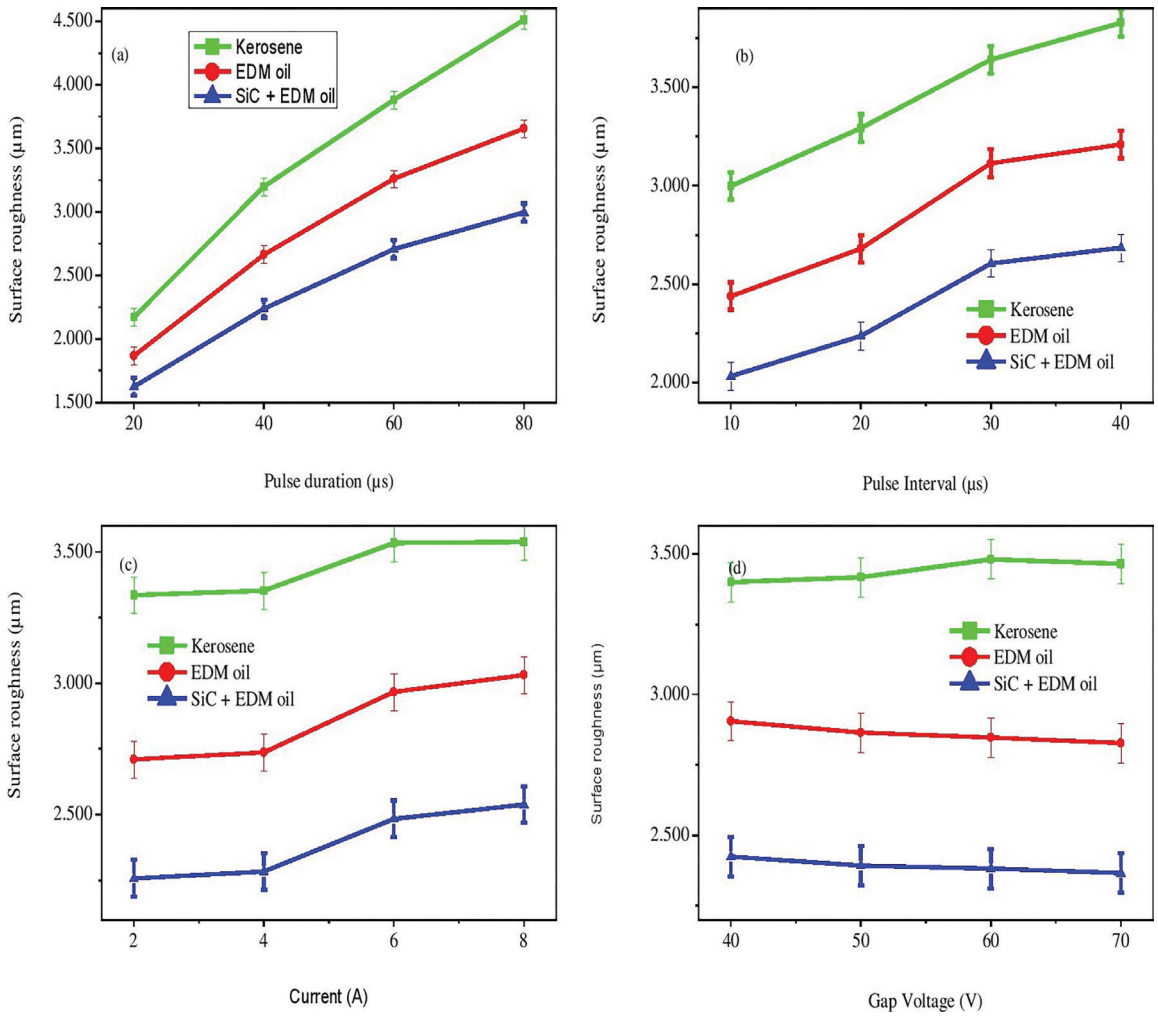

Figure 9: Effect of process parameters on SR for Kerosene, EDM oil and SiC + EDM oil: (a) T_{on}, (b) T_{off}, (c) I and (d) GV.

in mean values across several groups. The sum of squares, degree of freedom, and variance were chosen as the statistical parameters to be evaluated. To determine the difference between experimental data and mean value, the sum of squares was utilized. The mean square to Error term ratio was used to determine the F value [61]. The 95 percent confidence level was used. For analysis, the general linear model was chosen. For SiC mixed EDM oil, it was created in MINITAB software, as indicated in Table 5. The ANOVA was used to find the statistically significant factor based on the p value. Ton was discovered to be a significant factor for MRR and SR [62]. The standard deviation (S), R-squared, and R-squared adjusted values were used to judge the ANOVA models. The MRR, EWR, and SR showed lower standard deviations. The R-squared values for MRR and SR were greater than 90% in the model assessments, which was satisfactory. However, the R-squared adjusted values for EWR were also greater than 90%, which was a better result. Moreover, additional parameters were needed to produce the stronger model [63]. More than 90% of the MRR's R-squared and R-squared adjusted values were positive, which was a good sign that the model was robust. MRR and SR's experimental EWRs were small and allowable.

4.6. Quadratic modeling

Modeling is a statistical technique used to examine the connections between the process's dependent and independent variables, or its outputs and inputs [64]. As shown below, Microsoft Excel was used to make the quadratic models for MRR, EWR, and SR.

$$MRR = 0.00092 + 0.00011T_{on} + 9.66E^{-05}T_{off} + 6.2E^{-05}I - 2.3E^{-05}GV - 3.2E^{-07}T_{on}^{2} - 3.1E^{-07}T_{off}^{2} + 5.12E^{-06}I^{2} + 3.5E^{-07}GV^{2} - 3.1E^{-08}T_{on}T_{off}I - 7.1E^{-09}T_{on}IGV - 6.4E^{-08}T_{off}IGV + 7.43E^{-10}IGVT_{on}$$

R-Square = 0.997267; Adjusted R-Square = 0.986336; Standard Error = 0.000197.

$$EWR = 0.000295 + 2.58E^{-05}T_{on} + 1.71E^{-05}T_{off} - 1.4E^{-05}I + 3.95E^{-05}GV - 2E^{-07}T_{on}^{2} - 8.2E^{-07}T_{off}^{2} - 8.1E^{-06}I^{2} - 4E^{-07}GV^{2} - 5.1E^{-08}T_{on}T_{off}I + 4.14E^{-11}T_{on}IGV + 6.7E\text{-}08T_{off}IGV - 2.2E^{-09}IGVT_{on}$$

Table 5: ANOVA for SiC + EDM oil medium.

SOURCE	DF	SEQ SS	ADJ SS	ADJ MS	F	P
MATERIAL REMOVAL RATE (g/s)						
T_{on}	3	$3.89E^{-05}$	$3.89E^{-05}$	0.000013	114.48	0.001
T_{off}	3	$3.1E^{-06}$	$3.1E^{-06}$	0.000001	9.06	0.052
I	3	$2E^{-07}$	$2E^{-07}$	$1E^{-07}$	0.51	0.701
GV	3	0	0	0	0.04	0.989
Error	3	$3E^{-07}$	$3E^{-07}$	$1E^{-07}$		
Total	15	$4.25E^{-05}$				
S = 0.00033 R-Sq = 99.20% R-Sq(adj) = 96.00%						
ELECTRODE WEAR RATE (g/s)						
T_{on}	3	$1E^{-07}$	$1E^{-07}$	0	0.97	0.508
T_{off}	3	$4E^{-07}$	$4E^{-07}$	$1E^{-07}$	3.88	0.147
I	3	$2E^{-07}$	$2E^{-07}$	$1E^{-07}$	1.88	0.309
GV	3	$1E^{-07}$	$1E^{-07}$	0	1.14	0.459
Error	3	$1E^{-07}$	$1E^{-07}$	0		
Total	15	$8E^{-07}$				
S = 0.00017 R-Sq = 98.73% R-Sq(adj) = 93.65%						
SURFACE ROUGHNESS (µm)						
T_{on}	3	4.301	4.301	1.43367	59.99	0.004
T_{off}	3	1.13655	1.13655	0.37885	15.85	0.024
I	3	0.23737	0.23737	0.07912	3.31	0.176
GV	3	0.00708	0.00708	0.00236	0.1	0.955
Error	3	0.07169	0.07169	0.0239		
Total	15	5.75369				
S = 0.15 R-Sq = 98.75% R-Sq(adj) = 93.77%						

R-Square = 0.960352; Adjusted R-Square = 0.801759; Standard Error = 0.000104.

$$SR = 1.081818 + 0.046262T_{on} + 0.063295T_{off} + 0.176379I - 0.06793GV + 0.00022T_{on}^{2} - 0.00045T_{off}^{2} - 0.00219I^{2} + 0.000585GV^{2} + 7.2E\text{-}05T_{on}T_{off}I + 1.17E\text{-}06T_{on}IGV - 3.1E\text{-}05T_{off}IGV + 2.45E^{-06}IGVT_{on}$$

R-Square = 0.994176; Adjusted R-Square = 0.970878; Standard Error = 0.105686.

Here

T_{on} – pulse duration

T_{off} – pulse interval

I – current

GV – Gap voltage

Here, small S value, large R-squared value and large R-squared adjusted values were characteristics of well-fit models. The large R-Sq and R-Sq (adj) values provide the MRR, EWR, and SR models a good fit and high strength, and this model was utilised for further prediction. In a prior study, a comparable outcome was seen [65]. Table 6 displays the MRR, EWR, and SR expected and Error values. Owing to large R-Sq and large R-Sq (adj) values, it was discovered that experimental data and anticipated data values for MRR, EWR, and SR are in the fitted line. Table 7 shows the model factors and it was found that Mean Absolute Percentage Error (MAPE), coefficient of determination (R), and Root Mean Square Error (RMSE) were good because of low MAPE, RMSE, and high R.

4.7. To find the optimum process parameters using COPRAS

The COPRAS method was chosen because the response is related to the significance and value of a number of different options. The ease of use of this method is the primary advantage that it possesses. The MRR is chosen in this method in order to achieve the maximum possible benefit from the method, while the EWR and SR are chosen so as to achieve the minimum possible benefit. The outputs are formulated as a decision matrix using

Table 6: Predicted values for SiC powder added EDM oil.

S. NO.	PREDICTION USING QUADRATIC MODEL			ERROR % IN ACTUAL VS QUADRATIC MODEL		
	MRR	EWR	SR	MRR	EWR	SR
1	0.00174	0.00172	1.031	0.00005	0.00000	0.040
2	0.00256	0.00171	1.537	–0.00019	–0.00006	–0.122
3	0.00314	0.00158	1.891	0.00021	0.00007	0.107
4	0.00342	0.00142	2.053	–0.00004	–0.00001	–0.039
5	0.00372	0.00189	1.733	0.00005	0.00006	0.003
6	0.00438	0.00185	2.003	–0.00003	–0.00001	–0.001
7	0.00479	0.00122	2.668	–0.00003	0.00000	0.014
8	0.00497	0.00127	2.505	–0.00011	–0.00007	0.026
9	0.00543	0.00168	2.470	–0.00004	–0.00006	–0.005
10	0.0056	0.00153	2.623	0.00006	0.00000	–0.031
11	0.00604	0.00182	2.745	–0.00001	0.00000	0.017
12	0.00645	0.00118	3.024	0.00010	0.00007	–0.024
13	0.00655	0.00139	2.847	–0.00001	0.00003	0.016
14	0.00674	0.00146	2.949	–0.00002	–0.00005	–0.008
15	0.00682	0.0015	2.960	0.00000	0.00004	0.023
16	0.00731	0.0013	3.213	–0.00001	–0.00003	–0.017

Table 7: Quadratic modeling evaluations.

RESPONSES	QUADRATIC MODEL FACTORS		
	MAPE	RMSE	R
Material Removal Rate	0.00001	0.00000	1.0000
Electrode Wear Rate	0.00000	0.00000	0.99937
Surface Roughness	0.06250	0.00000	0.99937

Table 8: COPRAS for nano-SiC powder added EDM oil.

S. NO.	DECISION MATRIX			NORMALIZED MATRIX			WEIGHTED NORMALIZED MATRIX			BENEFICIAL CRITERIA, BI	NON-BENEFICIAL CRITERIA, CI	QI	UTILITY DEGREE, UD	RANK
	MRR	EWR	SR	MRR	EWR	SR	MRR	EWR	SR					
1	0.00180	0.00173	1.071	0.02255	0.07048	0.028	0.00902	0.02819	0.008	0.009	0.037	0.061	77.99	15
2	0.00237	0.00165	1.415	0.02980	0.06722	0.037	0.01192	0.02689	0.011	0.012	0.038	0.062	79.26	13
3	0.00335	0.00165	1.998	0.04208	0.06718	0.052	0.01683	0.02687	0.016	0.017	0.043	0.061	78.69	14
4	0.00338	0.00142	2.014	0.04242	0.05779	0.053	0.01697	0.02312	0.016	0.017	0.039	0.066	84.20	11
5	0.00377	0.00195	1.737	0.04738	0.07942	0.045	0.01895	0.03177	0.014	0.019	0.045	0.061	77.82	16
6	0.00435	0.00184	2.002	0.05462	0.07498	0.052	0.02185	0.02999	0.016	0.022	0.046	0.063	81.17	12
7	0.00476	0.00123	2.682	0.05978	0.05008	0.070	0.02391	0.02003	0.021	0.024	0.041	0.070	89.82	8
8	0.00486	0.00120	2.531	0.06100	0.04886	0.066	0.02440	0.01954	0.020	0.024	0.039	0.073	92.96	6
9	0.00539	0.00162	2.465	0.06761	0.06599	0.064	0.02704	0.02640	0.019	0.027	0.046	0.069	87.78	9
10	0.00567	0.00153	2.593	0.07111	0.06254	0.068	0.02844	0.02501	0.020	0.028	0.045	0.070	90.02	7
11	0.00604	0.00182	2.762	0.07575	0.07419	0.072	0.03030	0.02968	0.022	0.030	0.051	0.067	86.15	10
12	0.00655	0.00125	3.000	0.08226	0.05109	0.078	0.03290	0.02043	0.024	0.033	0.044	0.076	97.43	2
13	0.00654	0.00142	2.862	0.08209	0.05802	0.075	0.03284	0.02321	0.022	0.033	0.046	0.074	95.28	4
14	0.00672	0.00141	2.941	0.08433	0.05739	0.077	0.03373	0.02296	0.023	0.034	0.046	0.075	96.02	3
15	0.00682	0.00154	2.984	0.08557	0.06290	0.078	0.03423	0.02516	0.023	0.034	0.049	0.073	93.88	5
16	0.00730	0.00127	3.196	0.09166	0.05188	0.084	0.03666	0.02075	0.025	0.037	0.046	0.078	100.00	1

equation (6). The calculations are made to normalise the decision matrix and create a weighted-normalized decision matrix using equation (7) and equation (8), respectively. The calculations are made to find the value of the total benefit (MRR) and cost criteria (EWR and SR) using equation (9) and equation (10), respectively. Equation (11) is used to determine the proportional importance of each option. Equation (12) is used to find the degree of utility for every alternative. Finally, rank is formed based on the UD values. The above calculations are formed into tabular form, as shown in Table 8. The COPRAS strategy is used to enhance the performance indicators of the EDM process. Based on the results of COPRAS process, the rank arrangement of alternative is found from experimental number 1 to 16 as 15-13-14-11-16-12-8-6-9-7-10-2-4-3-5-1. The best combinations of inputs are found in run 16 with a 100% utility degree. Moreover, Run 1 is the worst alternative, with 77.99% utility degree. The optimal combinations are identified with a current of 8A, pulse duration of 80 µs, gap voltage of 60 V, and a pulse interval of 40 µs for improving the MRR, EWR, and SR.

4.8. Discussions with previous works

The work was to form a micron level square hole on AZ61Mg/B_4C composites using three different dielectric fluids via kerosene, EDM oil, and nano-SiC added EDM oil to improve the high MRR, low EWR, and low SR. To achieve the above objectives, the Taguchi-based Complex Proportional Assessment method was used. To achieve the micron level square hole on magnesium composite, the minimum square electrode was fabricated

Table 9: Compared with previous works.

S. NO.	APPROACHES	SAMPLE/ELECTRODE MATERIALS/DIELECRIC MEDIUM	CONDITIONS	MRR (g/s)	EWR (g/s)	SR (µm)
[67]	On increasing T_{on}	Mg/SiCp composites/Ø 10 mm Copper/Kerosene	T_{on} = 1000 µs, 200 µs T_{off} = 200 µs, 50 µs I = 10 A	0.0025	–	–
[30]	RSM approach	Al–Mg2Si/ Ø 5.5 mm Copper/Oil	T_{on} = 200 µs I = 15 A SV = 50 V	0.0009	–	–
[68]	GA approach	AA7075/2.5%TiC + 2.5%B_4C/ Ø 7 mm Copper/Kerosene	T_{on} = 12 µs I = 10–20 A SV = 70 V	0.0031	0.0009	–
[69]	TOPSIS approach	Al 6061+3% SiC+7 % B_4C/ Ø 10 mm Copper/EDM oil	T_{on} = 20 µs I = 9 A T_{off} = 50 µs	0.0001	0.0003	4.108
[70]	RSM–DFA method	AA7075+10 wt.% TiO_2/ Ø 12 mm Brass/kerosene	T_{on} = 899 µs I = 14 A T_{off} = 30 µs	0.008	–	4.97
[78]	TLBO method	Mg/nil/nil	T_{on} = 40 µs I = 1 A T_{off} = 9 µs	–	–	2.4
[79]	On adding Zinc particles	AZ31 Mg/copper/1 g/l zinc added dielectric medium	T_{on} = 16 µs I = 38 A T_{off} = 128 µs	–	–	5.77
[71]	GRA method	Mg/ Ø 0.5 mm Brass/Distilled water	T_{on} = 4 µs I = 5 A T_{off} = 3 µs	–	0.0187	–
[80]	Taguchi method	AZ31 Mg/copper/kerosene	T_{on} = 16 µs I = 38 A SV = 80 V	–	–	6.50
[72]	GRA and TOPSIS Approach	AZ31 Mg/copper/kerosene	T_{on} = 10 µs I = 3 A T_{off} = 5 µs	–	0.00007	3.2
Present work	On using COPRAS method	AZ61/7.5% B_4C composites/ 0.8 mm square copper electrode	T_{on} = 80 µs T_{off} = 40 µs I = 8 A GV = 60 V	0.00730	0.00127	3.196

using a vertical machining centre [66]. It was found that less than a 0.8 mm square electrode was unable to be formed using the vertical machining centre because of high workpiece deflection at the free end. Hence, a 0.8 mm square electrode was fabricated to machine AZ61Mg/B_4C composites using EDM. The MRR, EWR, and SR were studied with varying EDM process parameters and different dielectric medium, the MRR, EWR and SR were studied. The MRR for EDM was low generally. To improve the MRR, nano-SiC added EDM oil was proposed in this work. The presented works were compared with other works, as shown in Table 9. The MRR was dependent mainly on Ton, I, and DC factors. Hence, based on the machine limits and previous work, the process parameters were selected and the experiments were conducted. When compared to previous MRR works [30, 67–70], the current MRR values produced better results. Variations in results were due to more factors, such as density, specific heat, thermal conductivity, and melting point of workpiece and electrode materials. The current EWR outperformed the others [68, 69, 71, 72]. EWR was primarily proportional to c (specific heat), (thermal conductivity), and (melting point) [73]. The copper electrode has limited wear in the EDM. To reduce the copper wear, the EDM process parameters and different dielectric mediums were used to achieve low wear. Previous research discovered that increasing pulse duration [74], pulse interval [75], decreasing current [76], and using high melting point electrode material [77] reduced electrode wear. In comparison to kerosene's thermal conductivity (λ = 0.128 W/m k), EDM oil (λ = 120 W/m k) and SiC (λ = 83.6 W/m k) had higher thermal conductivity, which was used to improve the dielectric medium›s performance. Hence, the SiC mixed EDM oil produced a low EWR and a high MRR. The SR was dependent on crater formation in the machined surface. The EDM process parameters and dielectric medium were affecting the crater depth and width. Compared with other SRs [69–71, 78–80], the present result found that the high discharge conditions produced a low SR due to the presence of SiC-added EDM oil.

5. CONCLUSIONS

The purpose of this work is used to increase the material removal rate and reduces the electrode wear rate and surface roughness of AZ61Mg/B_4C composites by using kerosene, EDM oil and nano-SiC added EDM oil performance in EDM. The following statements have been made based on the experimental result and analysis.

- The nano-B_4C added AZ61 nanocomposites have a better bonding strength due to the new intermetallic phase β-$Mg_{17}Al_{12}$
- The nano-SiC added EDM oil produces a better result compared with kerosene and EDM oil based on the values of the interval plot.
- The both nano-SiC added EDM oil and the Taguchi based COPRAS method has used to enhance the performance measures.
- The pulse duration has highly affected the MRR, EWR and SR.
- The model values for MRR, EWR, and SR have an excellent fit for prediction based on the R-squared value and R-squared adjusted value.
- The COPRAS method has enhanced performance measures.
- The laser surface treated SiC nanopowder-added EDM oil can be used further for improving the performance measures.

6. ACKNOWLEDGMENTS

The authors are thanked the COVAI EDM at Coimbatore for using EDM facility.

7. BIBLIOGRAPHY

[1] PAULO DAVIM, J., CHARITIDIS, C.A., *Nanocomposites: materials, manufacturing and engineering*, Berlim, DeGruyter, 2013. doi: http://dx.doi.org/10.1515/9783110267426.

[2] PAULO DAVIM, J., *Nonconventional machining*, v. 7, Berlim, DeGruyter, 2023.

[3] PAULO DAVIM, J., *Nontraditional machining processes*, USA, Springer, 2013. doi: http://dx.doi.org/10.1007/978-1-4471-5179-1.

[4] BAINS, P.S., SIDHU, S.S., PAYAL, H.S., "Magnetic field assisted EDM: new horizons for improved surface properties", *Silicon*, v. 10, n. 4, pp. 1275–1282, 2018. doi: http://dx.doi.org/10.1007/s12633-017-9600-7.

[5] PAULO DAVIM, J., *Computational methods and production engineering*, USA, Elsevier, 2017.

[6] PAULO DAVIM, J., *Statistical and computational techniques in manufacturing*, USA, Springer, 2012. doi: http://dx.doi.org/10.1007/978-3-642-25859-6.

[7] PAULO DAVIM, J., *Design of experiments in production engineering*, USA, Springer, 2016. doi: http://dx.doi.org/10.1007/978-3-319-23838-8.

[8] PAULO DAVIM, J., CONCEIÇÃO ANTÓNIO, C.A., "Optimisation of cutting conditions in machining of aluminium matrix composites using a numerical and experimental model", *Journal of Materials Processing Technology*, v. 112, n. 1, pp. 78–82, 2001. doi: http://dx.doi.org/10.1016/S0924-0136(01)00551-9.

[9] PAULO DAVIM, J., CONCEIÇÃO ANTÓNIO, C.A., "Optimal drilling of particulate metal matrix composites based on experimental and numerical procedures", *International Journal of Machine Tools & Manufacture*, v. 41, n. 1, pp. 21–31, 2001. doi: http://dx.doi.org/10.1016/S0890-6955(00)00071-7.

[10] KANAGARAJAN, D., KARTHIKEYAN, R., PALANIKUMAR, K., *et al*., "Optimization of electrical discharge machining characteristics of WC/Co composites using non-dominated sorting genetic algorithm (NSGA-II)", *International Journal of Advanced Manufacturing Technology*, v. 36, n. 11–12, pp. 1124–1132, 2008. doi: http://dx.doi.org/10.1007/s00170-006-0921-8.

[11] MAGABE, R., SHARMA, N., GUPTA, K., *et al*., "Modeling and optimization of Wire-EDM parameters for machining of Ni55.8Ti shape memory alloy using hybrid approach of Taguchi and NSGA", *International Journal of Advanced Manufacturing Technology*, v. 102, n. 5–8, pp. 1703–1717, 2019. doi: http://dx.doi.org/10.1007/s00170-019-03287-z.

[12] BAINS, P.S., BAHRAMINASAB, M., SIDHU, S.S., *et al*., "On the machinability and properties of Ti–6Al–4V biomaterial with n-HAp powder–mixed ED machining", *Proceedings of the Institution of Mechanical Engineers. Part H, Journal of Engineering in Medicine*, v. 234, n. 2, pp. 232–242, 2020. doi: http://dx.doi.org/10.1177/0954411919891887. PMid:31804148.

[13] DHIMAN, S., SIDHU, S.S., BAINS, P.S., *et al*., "Mechanobiological assessment of Ti-6Al-4V fabricated via selective laser melting technique: a review", *Rapid Prototyping Journal*, v. 25, n. 7, pp. 1266–1284, 2019. doi: http://dx.doi.org/10.1108/RPJ-03-2019-0057.

[14] BHUI, A.S., SINGH, G., SIDHU, S.S., *et al*.,"Experimental investigation of optimal ED machining parameters for Ti-6Al-4V biomaterial",*Facta Universitatis, Series*, *Mechanical Engineering*, v. 16, n. 3, pp. 337–345, 2018.

[15] JAYAKUMAR, K., "Optimization of process parameters during EDM on inconel alloy 625", In: VIJAYAN, S., SUBRAMANIAN, N., SANKARANARAYANASAMY, K. (eds), *Trends in Manufacturing and Engineering Management. Lecture Notes in Mechanical Engineering. Springer, Singapore,* 2021, v. 784, pp. 897–904. doi: https://doi.org/10.1007/978-981-15-4745-4_77.

[16] JAYAKUMAR, K., MATHEW, J., JOSEPH, M.A., *et al*., "Synthesis and characterization of A356-Sic_p composite produced through vacuum hot pressing", *Materials and Manufacturing Processes*, v. 28, n. 9, pp. 991–998, 2013. https://doi.org/10.1080/10426914.2013.773012.

[17] SEKAR, K., MANOHAR, M., JAYAKUMAR, K., "Mechanical and tribological properties of A356/Al_2O_3/MoS_2 hybrid composites synthesized through combined stir and squeeze casting", In: LAKSHMI NARAYANAN, A., IDAPALAPATI, S., VASUDEVAN, M. (eds), *Advances in Materials and Metallurgy. Lecture Notes in Mechanical Engineering, Singapore, Springer,* v. 939, pp. 115–125, 2019. doi: https://doi.org/10.1007/978-981-13-1780-4_13.

[18] VISWANATHAN, R., RAMESH, S., SUBBURAM, V., "Measurement and optimization of performance characteristics in turning of Mg alloy under dry and MQL conditions", *Measurement*, v. 120, pp. 107–113, 2018. doi: http://dx.doi.org/10.1016/j.measurement.2018.02.018.

[19] GOPAL, P.M., PRAKASH, K.S., "Minimization of cutting force, temperature and surface roughness through GRA, TOPSIS and Taguchi techniques in end milling of Mg hybrid MMC", *Measurement*, v. 116, pp. 178–192, 2018. doi: http://dx.doi.org/10.1016/j.measurement.2017.11.011.

[20] SIDDESH KUMAR, N.G., SHIVA SHANKAR, G., BASAVARAJAPPA, S., *et al*., "Some studies on mechanical and machining characteristics of Al2219/n-B_4C/MoS_2 nano-hybrid metal matrix composites", *Measurement*, v. 107, pp. 1–11, 2017. doi: https://doi.org/10.1016/j.measurement.2017.05.003.

[21] DATTA, S., BISWAL, B., MAHAPATRA, S., "Machinability analysis of Inconel 601, 625, 718 and 825 during electro-discharge machining: on evaluation of optimal parameters setting", *Measurement*, v. 137, pp. 382–400, 2019. doi: http://dx.doi.org/10.1016/j.measurement.2019.01.065.

[22] WOJCIECHOWSKI, S., WIACKIEWICZ, M., KROLCZYK, G.M., "Study on metrological relations between instant tool displacements and surface roughness during precise ball end milling",*Measurement*, v. 129, pp. 686–694, 2018. doi: http://dx.doi.org/10.1016/j.measurement.2018.07.058.

[23] GOPAL, P.M., PRAKASH, K.S., JAYARAJ, S., "WEDM of Mg/CRT/BN composites: effect of materials and machining parameters", *Materials and Manufacturing Processes*, v. 33, n. 1, pp. 77–84, 2018. doi: http://dx.doi.org/10.1080/10426914.2017.1279316.

[24] SIVAIAH, P., CHAKRADHAR, D., "Performance improvement of cryogenic turning process during machining of 17-4 PH stainless steel using multi objective optimization techniques", *Measurement*, v. 136, pp. 326–336, 2019. doi: http://dx.doi.org/10.1016/j.measurement.2018.12.094.

[25] SATHISH, T., MOHANAVEL, V., ANSARI, K., *et al*., "Synthesis and characterization of mechanical properties and wire cut EDM process parameters analysis in AZ61 magnesium alloy+ B_4C+ SiC", *Materials (Basel)*, v. 14, n. 13, pp. 3689, 2021. doi: http://dx.doi.org/10.3390/ma14133689. PMid:34279259.

[26] MUNI, R.N., SINGH, J., KUMAR V., *et al*., "Parametric optimization of rice husk ash, copper, magnesium reinforced aluminium matrix hybrid composite processed by EDM", *ARPN Journal of Engineering and Applied Sciences*, v. 14, n. 22, pp. 3832–3839, 2019.

[27] PONAPPA, K., ARAVINDAN, S., RAO, P.V., *et al*., "The effect of process parameters on machining of magnesium nano alumina composites through EDM", *International Journal of Advanced Manufacturing Technology*, v. 46, n. 9–12, pp. 1035–1042, 2010. doi: http://dx.doi.org/10.1007/s00170-009-2158-9.

[28] KAVIMANI, V., PRAKASH, K.S., THANKACHAN T., "Multi-objective optimization in WEDM process of graphene–SiC-magnesium composite through hybrid techniques", *Measurement*, v. 145, pp. 335–349, 2019. doi: http://dx.doi.org/10.1016/j.measurement.2019.04.076.

[29] KAVIMANI, V., PRAKASH, K., SOORYA, T., *et al*., "Influence of machining parameters on wire electrical discharge machining performance of reduced graphene oxide/magnesium composite and its surface integrity characteristics", *Composites. Part B, Engineering*, v. 167, pp. 621–630, 2019. doi: http://dx.doi.org/10.1016/j.compositesb.2019.03.031.

[30] HOURMAND, M., FARAHANY, S., SARHAN, A.A., *et al*., "Investigating the electrical discharge machining (EDM) parameter effects on Al-Mg_2Si metal matrix composite (MMC) for high material removal rate (MRR) and less EWR–RSM approach", *International Journal of Advanced Manufacturing Technology*, v. 77, n. 5–8, pp. 831–838, 2015. doi: http://dx.doi.org/10.1007/s00170-014-6491-2.

[31] SIDHU, S.S., YAZDANI, M., "Comparative analysis of MCDM techniques for EDM of SiC/A359 composite", *Arabian Journal for Science and Engineering*, v. 43, n. 3, pp. 1093–1102, 2018. doi: http://dx.doi.org/10.1007/s13369-017-2726-5.

[32] SIDHU, S.S., BATISH, A., KUMAR, S., "Fabrication and electrical discharge machining of metal–matrix composites: a review", *Journal of Reinforced Plastics and Composites*, v. 32, n. 17, pp. 1310–1320, 2013. doi: http://dx.doi.org/10.1177/0731684413489366.

[33] SEO, Y.W., KIM, D., RAMULU, M., "Electrical discharge machining of functionally graded 15-35 vol% SiCp/Al composites", *Materials and Manufacturing Processes*, v. 21, n. 5, pp. 479–487, 2006. doi: http://dx.doi.org/10.1080/10426910500471482.

[34] MALHOTRA, P., SINGH, N.K., TYAGI, R.K., *et al*., "Comparative study of rotary-EDM, gas assisted-EDM, and gas assisted powder mixed-EDM of the hybrid metal matrix composite", *Advances in Materials and Processing Technologies*, v. 7, n. 1, pp. 27–41, 2021. doi: http://dx.doi.org/10.1080/2374068X.2020.1855398.

[35] HOURMAND, M., SARHAN, A.A., FARAHANY, S., *et al*., "Microstructure characterization and maximization of the material removal rate in nano-powder mixed EDM of Al-Mg2Si metal matrix composite – ANFIS and RSM approaches", *International Journal of Advanced Manufacturing Technology*, v. 101, n. 9–12, pp. 2723–2737, 2019. doi: http://dx.doi.org/10.1007/s00170-018-3130-3.

[36] GOPALAKANNAN, S., SENTHILVELAN, T., "Application of response surface method on machining of Al–SiC nano-composites", *Measurement*, v. 46, n. 8, pp. 2705–2715, 2013. doi: http://dx.doi.org/10.1016/j.measurement.2013.04.036.

[37] SINGH, B., KUMAR, J., KUMAR, S., "Investigation of the tool wear rate in tungsten powder-mixed electric discharge machining of AA6061/10% SiCp composite", *Materials and Manufacturing Processes*, v. 31, n. 4, pp. 456–466, 2016. doi: http://dx.doi.org/10.1080/10426914.2015.1025965.

[38] MOHAL, S., KUMAR, H., "Parametric optimization of multiwalled carbon nanotube-assisted electric discharge machining of Al-10% SiCp metal matrix composite by response surface methodology", *Materials and Manufacturing Processes*, v. 32, n. 3, pp. 263–273, 2017. doi: http://dx.doi.org/10.1080/10426914.2016.1140196.

[39] KUNG, K.Y., HORNG, J.T., CHIANG, K.T., "Material removal rate and electrode wear ratio study on the powder mixed electrical discharge machining of cobalt-bonded tungsten carbide", *International Journal of Advanced Manufacturing Technology*, v. 40, n. 1–2, pp. 95–104, 2009. doi: http://dx.doi.org/10.1007/s00170-007-1307-2.

[40] ASSARZADEH, S., GHOREISHI, M., "A dual response surface-desirability approach to process modeling and optimization of Al_2O_3 powder-mixed electrical discharge machining (PMEDM) parameters", *International Journal of Advanced Manufacturing Technology*, v. 64, n. 9–12, pp. 1459–1477, 2013. doi: http://dx.doi.org/10.1007/s00170-012-4115-2.

[41] JAMESON, E.C., *Electrical discharge machining*, Southfield, Society of Manufacturing Engineers, 2001.

[42] PRAMANIK, A., "Developments in the non-traditional machining of particle reinforced metal matrix composites", *International Journal of Machine Tools & Manufacture*, v. 86, pp. 44–61, 2014. doi: http://dx.doi.org/10.1016/j.ijmachtools.2014.07.003.

[43] SENTHILKUMAR, V., OMPRAKASH, B.U., "Effect of titanium carbide particle addition in the aluminium composite on EDM process parameters", *Journal of Manufacturing Processes*, v. 13, n. 1, pp. 60–66, 2011. doi: http://dx.doi.org/10.1016/j.jmapro.2010.10.005.

[44] DANESHMAND, S., MASOUDI, B., "Investigation of weight percentage of alumina fiber on EDM of Al/Al_2O_3 metal matrix composites", *Silicon*, v. 10, n. 3, pp. 1003–1011, 2018. doi: http://dx.doi.org/10.1007/s12633-017-9562-9.

[45] BHUYAN, R., ROUTARA, B., "Optimization the machining parameters by using VIKOR and Entropy Weight method during EDM process of Al–18% SiCp Metal matrix composite", *Decision Science Letters*, v. 5, pp. 269–282, 2016. doi: http://dx.doi.org/10.5267/j.dsl.2015.11.001.

[46] ROUTARA, B.C., BHUYAN, R.K., PARIDA, A.K., "Application of the entropy weight and TOPSIS method on Al–12% SiC Metal Matrix Composite during EDM", *International Journal of Manufacturing, Materials, and Mechanical Engineering*, v. 4, n. 4, pp. 49–63, 2014. doi: http://dx.doi.org/10.4018/ijmmme.2014100104.

[47] SINGH, S., YEH, M.F., "Optimization of abrasive powder mixed EDM of aluminum matrix composites with multiple responses using gray relational analysis", *Journal of Materials Engineering and Performance*, v. 21, n. 4, pp. 481–491, 2012. doi: http://dx.doi.org/10.1007/s11665-011-9861-z.

[48] VELMURUGAN, C., SUBRAMANIAN, R., THIRUGNANAM, S., *et al*., "Experimental investigations on machining characteristics of Al 6061 hybrid metal matrix composites processed by electrical discharge machining", *International Journal of Engineering Science and Technology*, v. 3, n. 8, pp. 87–101, 2011. doi: http://dx.doi.org/10.4314/ijest.v3i8.7.

[49] KANNAN, V.S., LENIN, K., SRINIVASAN, D., *et al*., "Investigation on laser square hole drilling of AA7475/SiC/ZrSiO4 composites", *Silicon*, v. 14, pp. 4557–4574, 2022. doi: https://doi.org/10.1007/s12633-021-01252-8.

[50] KOSTKA, A., COELHO, R.S., DOS SANTOS, J., *et al*., "Microstructure of friction stir welding of aluminium alloy to magnesium alloy", *Scripta Materialia*, v. 60, n. 11, pp. 953–956, 2009. doi: http://dx.doi.org/10.1016/j.scriptamat.2009.02.020.

[51] BEHNAMIAN, Y., SERATE, D., AGHAIE, E., *et al*., "Tribological behavior of ZK60 magnesium matrix composite reinforced by hybrid MWCNTs/B4C prepared by stir casting method", *Tribology International*, v. 165, pp. 107299, 2022. doi: http://dx.doi.org/10.1016/j.triboint.2021.107299.

[52] JAYAMATHY, M., KAILAS, S.V., KUMAR, K., *et al*., "The compressive deformation and impact response of a magnesium alloy: influence of reinforcement", *Materials Science and Engineering: A*, v. 393, n. 1–2, pp. 27–35, 2005. doi: https://doi.org/10.1016/j.msea.2004.09.070.

[53] SODICK INC., *Instruction Manual, Sodick Wire-Cut EDM PGM WHITE 3 AG Series (Version 2.0)*, Schaumburg, 2012.

[54] PATEL, K.M., PANDEY, P.M., RAO, P.V., "Determination of an optimum parametric combination using a surface roughness prediction model for EDM of Al2O3/SiCw/TiC ceramic composite", *Materials and Manufacturing Processes*, v. 24, n. 6, pp. 675–682, 2009. doi: http://dx.doi.org/10.1080/10426910902769319.

[55] MATA, F., BEAMUD, E., HANAFI, I., *et al*., "Multiple regression prediction model for cutting forces in turning carbon-reinforce PEEK CF30", *Advances in Materials Science and Engineering*, v. 2010, pp. 824098, 2010. doi: http://dx.doi.org/10.1155/2010/824098.

[56] SHARSAR, R., GHOSH, S., MANDAL, M.C., *et al*., "Optimum experimental setup of EDM using entropy coupled MCDM techniques", In: TYAGI, M., SACHDEVA, A., SHARMA, V. (eds), *Optimization Methods in Engineering. Lecture Notes on Multidisciplinary Industrial Engineering, Singapore, Springer*, pp. 549–566, 2021. doi: http://dx.doi.org/10.1007/978-981-15-4550-4_35.

[57] BONNY, K., DE BAETS, P., VLEUGELS, J., *et al*., "EDM machinability and frictional behavior of ZrO2-WC composites", *International Journal of Advanced Manufacturing Technology*, v. 41, pp. 1085–1093, 2009. doi: http://dx.doi.org/10.1007/s00170-008-1551-0.

[58] RAMESH, S., JENARTHANAN, M.P., BHUVANESH KANNA, A.S., "Experimental investigation of powder-mixed electric discharge machining of AISI P20 steel using different powders and tool materials", *Multidiscipline Modeling in Materials and Structures*, vol. 14, no. 3, pp. 549–566, 2018. doi: https://doi.org/10.1108/MMMS-04-2017-0025.

[59] WANG, C.C., YAN, B.H., "Blind-hole drilling of Al2O3/6061Al composite using rotary electro-discharge machining", *Journal of Materials Processing Technology*, v. 102, n. 1–3, pp. 90–102, 2000. doi: http://dx.doi.org/10.1016/S0924-0136(99)00423-9.

[60] MOHAN, B., RAJADURAI, A., SATYANARAYANA, K.G., "Effect of SiC and rotation of electrode on electric discharge machining of Al–SiC composite", *Journal of Materials Processing Technology*, v. 124, n. 3, pp. 297–304, 2002. doi: http://dx.doi.org/10.1016/S0924-0136(02)00202-9.

[61] RAMANUJAM, N., DHANABALAN, S., RAJ KUMAR, D., *et al*., "Investigation of micro-hole quality in drilled CFRP laminates through CO_2 laser", *Arabian Journal for Science and Engineering*, v. 46, pp. 7557–7575, 2021. doi: http://dx.doi.org/10.1007/s13369-021-05505-x.

[62] RAJ KUMAR, D., JEYAPRAKASH, N., CHE-HUA YANG *et al*., "Optimization of drilling process on carbon-fiber reinforced plastics using genetic-algorithm", *Surface Review and Letters,* v. 28, n. 03, pp. 2050056, 2021. doi: https://doi.org/10.1142/S0218625X20500560.

[63] CHIENG, B.W., IBRAHIM, N.A., YUNUS, W.W., "Optimization of tensile strength of poly (lactic acid)/graphene nanocomposites using response surface methodology", *Polymer-Plastics Technology and Engineering*, v. 51, n. 8, pp. 791–799, 2012. doi: http://dx.doi.org/10.1080/03602559.2012.663043.

[64] RAJ KUMAR, D., RANJITHKUMAR, P., SATHIYANARAYANAN, C., "Optimization of machining parameters on microdrilling of CFRP composites by Taguchi based desirability function analysis", *Indian Journal of Engineering and Materials Sciences*, v. 24, pp. 331–338, 2017.

[65] MUTHURAMAN, V., RAMAKRISHNAN, R., SUNDARAVADIVU, K., *et al*., "Predicting surface roughness of WEDMedWc-Co composite using box-behnken response surface method", *Advanced Materials Research,* v. 651, pp. 361–366, 2013. doi: http://dx.doi.org/10.4028/www.scientific.net/AMR.651.361.

[66] KUMAR, P.V., VIVEK, J., SENNIANGIRI, N., *et al*., "A study of added sic powder in kerosene for the blind square hole machining of cfrp using electrical discharge machining", *Silicon*, v. 14, n. 4, pp. 1831–1849, 2022. doi: http://dx.doi.org/10.1007/s12633-021-01243-9.

[67] ARUNKUMAR, L., RAGHUNATH, B.K., "Electro discharge machining characteristics of Mg/SiCP metal matrix composites by powder metallurgy (P/M) techniques", *IACSIT International Journal of Engineering and Technology*, v. 5, n. 5, pp. 4332–4338, 2013.

[68] PONAPPA, K., SASIKUMAR, K.S.K., SAMBATHKUMAR, M., *et al*., "Multi-objective optimization of EDM process parameters for machining of hybrid aluminum metal matrix composites (al7075/tic/b4c) using genetic algorithm", *Surface Review and Letters*, v. 26, n. 10, pp. 1950071, 2019. doi: http://dx.doi.org/10.1142/S0218625X19500719.

[69] BODUKURI, A.K., KESHA, E., "Multi-attribute optimization of EDM process parameters for machining of SiC and B4C particle reinforced Al 6061 metal matrix composite adopting TOPSIS method", *International Journal of Advanced Technology and Engineering Exploration*, v. 8, n. 79, pp. 735–752, 2021. doi: http://dx.doi.org/10.19101/IJATEE.2021.874132.

[70] ALAGARSAMY, S.V., RAVICHANDRAN, M., SARAVANAN, H., "Development of mathematical model for predicting the electric erosion behavior of TiO2 Filled Al-Zn-Mg-Cu (AA7075) alloy composite using RSM-DFA method", *Journal of Advanced Manufacturing Systems*, v. 20, n. 01, pp. 1–26, 2021. doi: http://dx.doi.org/10.1142/S0219686721500013.

[71] MEEL, R., SINGH, V., KATYAL, P., *et al*., "Optimization of process parameters of micro-EDD/EDM for magnesium alloy using Taguchi based GRA and TOPSIS method", *Materials Today: Proceedings*, v. 51, pp. 269–275, 2022. doi: http://dx.doi.org/10.1016/j.matpr.2021.05.287.

[72] SOMASUNDARAM, M., KUMAR, J.P., "Multi response optimization of EDM process parameters for biodegradable AZ31 magnesium alloy using TOPSIS and grey relational analysis", *Sadhana*, v. 47, n. 3, pp. 1–14, 2022. doi: http://dx.doi.org/10.1007/s12046-022-01908-0.

[73] NAVEEN ANTHUVAN, R., KRISHNARAJ, V., "Effect of coated and treated electrodes on Micro-EDM characteristics of Ti-6Al-4V", *Journal of the Brazilian Society of Mechanical Sciences and Engineering*, v. 42, p. 517, 2020. doi: http://dx.doi.org/10.1007/s40430-020-02578-x.

[74] DAVIS, R., SINGH, A., DEBNATH, K., *et al*., "Enhanced micro-electric discharge machining-induced surface modification on biomedical Ti-6Al-4V alloy", *Journal of Manufacturing Science and Engineering*, v. 144, n. 7, pp. 071002, 2022. doi: http://dx.doi.org/10.1115/1.4053110.

[75] KUPPAN, P., NARAYANAN, S., OYYARAVELU, R., *et al*., "Performance evaluation of electrode materials in electric discharge deep hole drilling of Inconel 718 superalloy", *Procedia Engineering*, v. 174, pp. 53–59, 2017. doi: http://dx.doi.org/10.1016/j.proeng.2017.01.141.

[76] MARADIA, U., KNAAK, R., DAL BUSCO, W., *et al*., "A strategy for low electrode wear in meso–micro-EDM", *Precision Engineering*, v. 42, pp. 302–310, 2015. doi: http://dx.doi.org/10.1016/j.precisioneng.2015.06.005.

[77] AAS, K.L., "Performance of two graphite electrode qualities in EDM of seal slots in a jet engine turbine vane", *Journal of Materials Processing Technology*, v. 149, n. 1–3, pp. 152–156, 2004. doi: http://dx.doi.org/10.1016/j.jmatprotec.2004.02.005.

[78] KUMARI, S., SONIA, P., SINGH, B., *et al*., "Optimization of surface roughness in EDM of pure magnesium (Mg) using TLBO", *Materials Today: Proceedings*, v. 26, pp. 2458–2461, 2020. doi: http://dx.doi.org/10.1016/j.matpr.2020.02.523.

[79] ABDUL-RANI, A.M., RAZAK, M.A., LITTLEFAIR, G., *et al*., "Improving EDM process on AZ31 magnesium alloy towards sustainable biodegradable implant manufacturing", *Procedia Manufacturing*, v. 7, pp. 504–509, 2017. doi: http://dx.doi.org/10.1016/j.promfg.2016.12.057.

[80] RAZAK, M.A., ABDUL-RANI, A.M., RAO, T.V.V.L.N., *et al*., "Electrical discharge machining on biodegradable AZ31 magnesium alloy using Taguchi method", *Procedia Engineering*, v. 148, pp. 916–922, 2016. doi: http://dx.doi.org/10.1016/j.proeng.2016.06.501.